



# Hydrogeochemical characterization and water quality assessment in parts of Indo-Gangetic Plain: An insight into the controlling processes

Ilma Arshad<sup>1</sup> · Rashid Umar<sup>1</sup>

Received: 2 November 2023 / Accepted: 25 March 2024 / Published online: 12 April 2024  
© The Author(s), under exclusive licence to Springer Nature Switzerland AG 2024

## Abstract

This study provides a comprehensive evaluation of groundwater chemistry, with a specific emphasis on characterizing the primary hydrogeochemical mechanism that is acting on the groundwater system in parts of Shahjahanpur, Uttar Pradesh (U.P.), India. For the said purposes, 54 groundwater samples from shallow and deep wells and 7 river water samples were examined for physico-chemical parameters in pre-monsoon (PRMS) and post-monsoon (POMS) seasons, 2019. The analysis of seasonal variations in the physico-chemical parameters conducted through one-way ANOVA statistical approach, unveiled that most of the parameters do not depict any significant seasonal fluctuations. Hydrogeochemically, groundwater was predominantly of Ca + Mg-HCO<sub>3</sub> type. Gibbs and other bivariate plots elucidated that silicate weathering dominantly influences the groundwater chemistry with ion exchange process also affecting it. The results of silica geothermometry revealed that groundwater descending from deeper depth have higher silica content, thus reflecting greater rock-water interaction at relatively higher temperature as compared to the one with lesser silica content. Relationship of SiO<sub>2</sub> with Cl and TDS indicates the involvement of both anthropogenic causes and geogenic mechanisms in regulating groundwater chemistry. Schoeller semi-logarithmic diagram illustrates similar fluctuations in concentrations of most of the major ions between river and groundwater suggesting the likelihood of interaction. The groundwater quality evaluation through water quality index indicates that water sourced from deeper wells is preferable for drinking. The evaluation of Sodium Adsorption Ratio, Kelley's Ratio and Residual Sodium Carbonate for irrigational use and Larson-Skold Index for industrial use indicates the appropriateness of both surface and groundwater for respective applications.

**Keywords** Hydrogeochemistry · Surface-groundwater interaction · Silica geothermometry · Conceptual model · Groundwater quality

## Introduction

The depletion and pollution of water resources has become a global issue posing threat to its long-term sustainability (Mays 2013). The policy makers in several countries have gradually switched over groundwater resources to fulfil the water demands of their inhabitants, due to pervasive exploitation of surface water and its degraded quality (Giordano 2009). The current global groundwater withdrawal rate is 982 km<sup>3</sup>/year which is expected to rise with increasing world's population (Mukherjee et al. 2021). In several

countries, the groundwater abstraction has already surpassed the recharge rates, thus leading to over-exploited aquifers. Currently, India is the largest groundwater consumer followed by United States and China (Mukherjee 2018). It is projected that the global population under water stress will rise to 2.7 billion by 2025 and India will be classified as 'water stressed' region meaning that water needs exceed its availability. Adding to the woes is rising contamination of groundwater. In water quality index, India occupies 120th rank among the 122 countries with approximately 70% of water being contaminated (NITI Ayog 2018). Taken together, these stresses can considerably raise the costs associated with water supply system and without timely intervention, may impact human health (Howard and Gelo 2002). Thus, the assessment and protection of groundwater quality is vital for ensuring sustainable water resources and safeguarding human and environmental health.

✉ Rashid Umar  
rashidumar7@gmail.com

<sup>1</sup> Department of Geology, Aligarh Muslim University, Aligarh 202002, Uttar Pradesh, India

The groundwater quality varies as a function of physico-chemical parameters and their inter-ionic relationship which in turn are affected by both geogenic and anthropogenic factors (Misstear et al. 2022; Ganiyu et al. 2023; Arshad and Umar 2023). The combined influence of these factors on groundwater quality is often intricate and site-specific. The geologic and hydrogeologic diversity of the region creates a complex hydrological setting, where groundwater undergoes intricate chemical interactions as it percolates through sediments and aquifers. Therefore, to ensure the sustainable groundwater utilization, it is imperative to delve deep into the hydrogeochemical characteristics, their spatial and temporal variations and governing processes that alters the groundwater quality (Nzama et al. 2021). Moreover, anthropogenic activities, such as intense agriculture, urbanization, and industrialization, can introduce a plethora of contaminants into the groundwater, posing significant risks to human and the environmental health (Arshad and Umar 2020). Various threats may manifest across a spectrum of spatial and temporal scales and requires appropriate monitoring strategies (Khokhar et al. 2023; Lapworth et al. 2023). Over the past few decades, several researchers have focused on the effective groundwater monitoring tools like the water quality index (WQI) models which enables the analysis of extensive water quality datasets to generate a single value that gives an idea of the overall water quality and aid in effective groundwater management (Parween et al. 2022; Sajib et al. 2023; Shaibur et al. 2023; Uddin et al. 2021, 2023a, b, c). Moreover, extensive investigations have also been carried out at both global and national levels to explore the role of hydrogeochemical processes accountable for alterations in the groundwater quality (Rouxel et al. 2011; Saba and Umar 2016; Yang et al. 2016; Zhang et al. 2017; Pazand et al. 2018; Ahmad et al. 2019; Li et al. 2019; Arumugam et al. 2021; Sinha et al. 2023). However, in various regions, including the current study area Shahjahanpur, there is still a need to explore comprehensive information on this aspect.

Various researchers have evaluated the water quality of Shahjahanpur. According to a study of Central Groundwater Board (CGWB 2013), the primary groundwater problems in Shahjahanpur include decreasing water levels specifically in urban areas and the occurrence of arsenic in few regions. Khan et al. (2015a) linked the deteriorating groundwater quality in this region with escalated anthropogenic activities, as well as the swift processes of urbanization and industrialization. Khan et al. (2016) assessed the water quality of river Garrah flowing in the area and revealed that the degradation of the river water had resulted from urban expansion and industrial development along its course. As per a study of Rajmohan and Amarasinghe (2016), the quality of

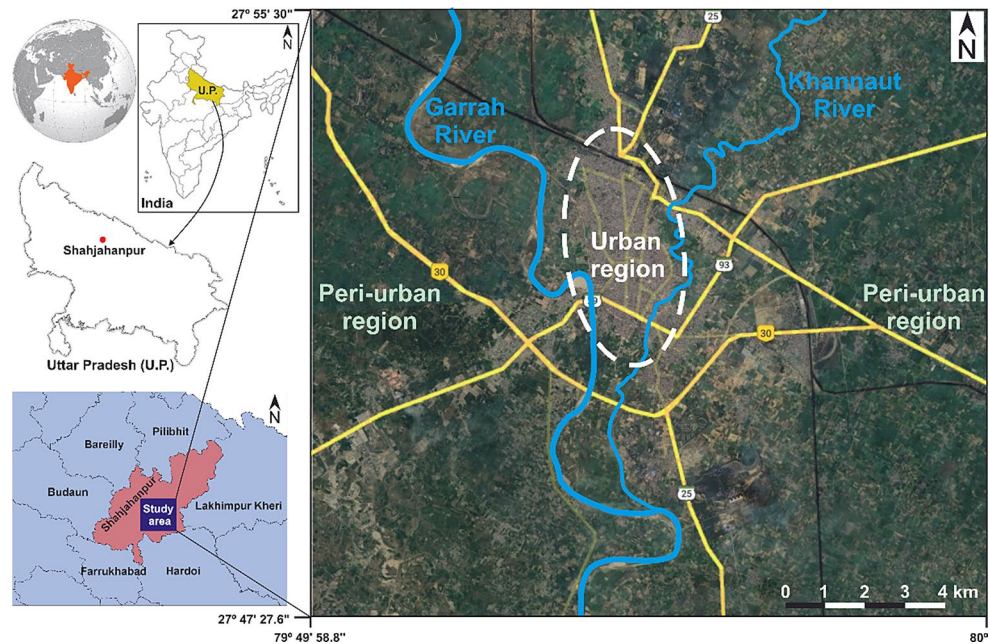
groundwater in the region was adversely affected by  $\text{NO}_3$ , Fe, Mn and As pollution.

Although, all the above research's highlight the deteriorating groundwater quality in the region, but lacks a systematic investigation on deciphering the primary hydrogeochemical processes that are operating within the area and are accountable for acquired groundwater composition and ultimately its quality. Furthermore, a detailed examination of water quality for its utility for diverse uses has not been thoroughly conducted. Therefore, the prime objectives of this study are: (a) delineation of major hydrogeochemical processes acting on the groundwater regime; (b) identification of the comparative influences of geogenic processes and anthropogenic factors acting on the aquifer system using silica values; (c) water quality assessment for its optimal utilization for drinking, irrigational and industrial use by employing various conventional indices. In summary, the outcomes of this research will address the current research gap by not only offering initial insights into hydrogeochemical processes, but also aiding the policy-makers in identifying areas where groundwater is more susceptible to pollution. This, in turn will enables the implementation of remedial measures to safeguard the water resource in the region. Also, the determination and implications of silica values in inferring the roles of geogenic and anthropogenic factors in governing the groundwater chemistry has been attempted afresh in the study area, thereby making it distinct from previous researches carried out in this region.

## Study area

The current work was conducted in the city of Shahjahanpur and its outskirts regions, located in the west-central region of U.P. The study encompasses an area of approximately 244 square kilometres, spanning the latitudinal and longitudinal range from  $27^\circ 47' 27.6''$  to  $27^\circ 55' 30''$  N and  $79^\circ 49' 58.8''$  to  $80^\circ$  E respectively (Fig. 1). The central city region which is densely urbanized has been designated as urban region while the surrounding outskirt areas are considered as peri-urban region for this study (Fig. 1). Khannaut and Garrah, both of which are the tributaries of river Ramganga, flows through the study area. The region experiences a subtropical and sub-humid climatic conditions with dry hot summers, dry winters and a humid monsoon season. The temperature during summer ranges from  $21.4^\circ\text{C}$  to  $40.5^\circ\text{C}$ , while in winter, it varies between  $8.5^\circ\text{C}$  to  $28.6^\circ\text{C}$ . The district has experienced an average annual rainfall of 759 mm from 2011 to 2020 (CGWB 2021). The region is renowned for both its agricultural activities and industrial enterprises. Principal monsoon crops are millet, paddy, sorghum and maize while the winter crops are gram, wheat, barley, oil

**Fig. 1** Map depicting the study area's geographical position and the classification of peri-urban and urban regions within it



seeds and pulses. The major industries located in the area are paper-pulp industry, sugar mill, thermal power plant, clothing and a fertilizer industry (CGWB 2021).

The area forms a part of Central Ganga Plain and is marked by a consistent flat topography that generally slopes towards the south and southeast. It depicts very less topographic variations and is nearly a flat terrain with ground elevation varying from 148 to 172 m above mean sea level (m amsl).

## Geology

From a geological perspective, the area is underlain by Quaternary alluvial deposits, with a thickness ranging from 400 to 600 m. The surface geology is shown in Fig. 2. These in turn are deposited over the Siwalik Supergroup, that unconformably overlays the Vindhyan Supergroup. The Siwaliks and Vindhyan Supergroups are not exposed in the study area. The Quaternary alluvium deposits comprise of primarily two formations i.e. Older Alluvium of Middle to Upper Pleistocene age and Newer Alluvium of Holocene age. The Newer Alluvium is found along the courses of Garrah and Khannaut rivers forming wedge shaped cover and comprised of sand, silt with thin clay lenses. The Older Alluvium comprised of oxidized silt, clay and sand with subordinate calc-concretions (Fig. 2). The generalized stratigraphic succession is provided in Table 1.

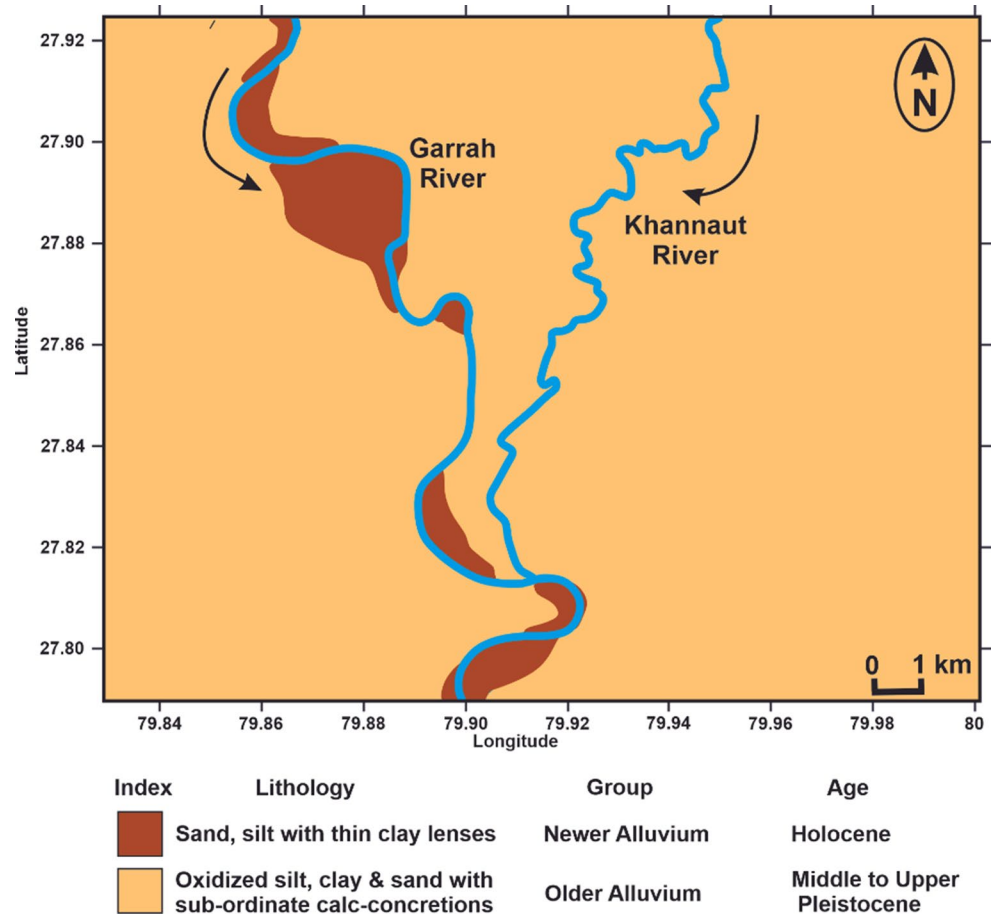
## Hydrogeology

CGWB had drilled a total of 10 exploratory wells in Shahjahanpur mainly within the older alluvium i.e. upto a maximum

depth of 456 m below ground level (m bgl) and identified three groups of aquifers down to this depth. The bottom depth range of the first aquifer in meters below ground level is from 90 to 130, second aquifer is 170 to 235 and third aquifer is beyond 300. In shallow aquifers, the groundwater exists in unconfined conditions and is tapped by hand-pumps and shallow borewells. The deep bore wells tap 30 to 40 m thickness in this aquifer in between the depth of 70 to 130 m, with discharge of 144 to 216 m<sup>3</sup>/hour. Groundwater exists under semi-confined to confined conditions in case of deep aquifers (CGWB 2013, 2021).

To attain a thorough comprehension of the lithological framework and the sub-surface configuration of the aquifer system, the lithological data of different boreholes were collected from the Uttar Pradesh Jal Nigam, Shahjahanpur and Central Groundwater Board, Bareilly for preparing the fence diagram (Fig. 3). The locations of the boreholes are illustrated in Fig. 4. The fence diagram shows the presence of a top persistent surface silty clay capping with thickness ranging from 3 to 5 m throughout the area. This layer is followed by a clay layer with calc-concretions. Below this layer lies two sand zones i.e. upper sand zone and lower sand zone with thickness ranging from 23 to 66 m and 13 to 69 m respectively. These two zones are separated from each other by sub-regional layer of clay with occasional calcareous concretions. The upper and lower sand zones are intervened by few clay lenses with calcareous concretions in north central and south western parts. Below these sand zones, lies a clay layer with thickness ranging from 3 to 20 m. This layer is relatively thicker in the western region in contrast to the eastern part. The clay layer occurs in lenticular form in the upper part while at deeper levels, it acquires

**Fig. 2** Map illustrating the study area geology (CGWB 2021)



a sub-regional character. The aquifer is chiefly comprised of fine, medium and coarse-grained sand. By and large these aquifers appear to merge with each other and behave as a single bodied aquifer system.

## Methodology

In order to obtain an inclusive understanding of water quality, a total of 54 and 7 samples were collected from groundwater and river water respectively. Out of the 54 groundwater samples, the number of samples collected from shallow wells of peri-urban area were 26 while the shallow and deep wells samples from urban area were 21 and 7 respectively (Fig. 4). It's crucial to emphasize that deep well samples were not collected from the peri-urban region due to the unavailability and non-operational status of such wells in that area. The shallow well samples were taken from hand-pumps and shallow bore wells while deep well samples were taken from deep bore wells. The depth of shallow and deep wells varied between 31–40 m and 70–130 m respectively as verified by the private well operators and lithological logs data of bore holes during the field visit. Samples were taken at varying depths to analyze the

vertical variations in groundwater quality. These samples were then subsequently analyzed for physico-chemical parameters during pre-monsoon season (the period before the onset of monsoon) and post-monsoon season (the period after monsoon), 2019.

Sampling was carried out on the existing wells following a grid sampling method, where the area was divided into numerous grids, each spanning an area of approximately 3 square kilometres, to achieve a consistent coverage of the entire study area. An attempt has been made to select the monitoring well from each grid. The samples obtained from shallow wells exceeds the deep wells as hand-pumps were more prevalent in comparison to the deep bore wells. Moreover, in 7 urban sites, hand-pumps as well as deep bore wells were located in close proximity, consequently, the samples from both shallow (27; 28; 29; 30; 32; 34; and 36) and deep wells (D1; D2; D3; D4; D5; D6 and D7) were collected from these locations. This approach has resulted in the overlapping of samples at these specific sites (Fig. 4). The sample collection was done after 5 to 10 min of pumping in a well-rinsed 1 L polyethylene bottle to facilitate the stagnant water removal from the well assembly. To prevent any contamination, the sampling bottles were rinsed with groundwater before sample collection. Well locations, their

**Table 1** Generalized stratigraphic succession of the area (CGWB 2013)

| Lithology   | Geological units  | Age                         |
|---|---|-----------------------------|
| Recent Alluvium (5–7 m thick)<br>Fluvial sediments; fine to medium loose micaceous sand with small amount of silt                         | Newer Alluvium  | Holocene                    |
| Terrace Alluvium with 2–8 m thick-cyclic sequence of grey coloured silt, micaceous sand and clay.   |   |                             |
| ----- Discontinuity -----   |   |                             |
| 400 to ~600 m thick multiple polycyclic fining upward sequence of oxidized silt, clay and sand with subordinate calc-concretions at depth | Older Alluvium  | Middle to Upper Pleistocene |
| ----- Discontinuity -----   |   |                             |
| > 1100 to ~2700 m thick sequence of sand/sandstone and clay/claystone   | Siwalik Supergroup (Upper Siwalik, Middle Siwalik and Lower Siwalik)- not exposed in the area | Tertiary                    |
| ~~~~~ Unconformity ~~~~~  |   |                             |
| Pre-Tertiary Basement rocks of Mesozoic/Precambrian Vindhyan Supergroup (not exposed in the area)   |   |                             |

latitude and longitude were taken by GPS. Depth to water level was taken with dip meter in both the sampling periods. In PRMS, 2019, it varied from 2.35 to 7.69 m below ground level (m bgl) for peri-urban region while 12.88 to 17.46 m bgl for urban region (Supplementary Fig. 1a). In POMS, 2019, it varied from 1.83 to 7.12 m bgl for peri-urban region, whereas for urban area, it varied from 12.75 to 17.57 m bgl respectively (Supplementary Fig. 1b). Further, the water table contour map was also prepared for POMS, 2019 to identify the groundwater flow direction (Supplementary Fig. 2). As per CGWB 2013 and 2021; the trend of regional groundwater flow typically follows a northeast to southwest direction. However, the water table contour map (Supplementary Fig. 2) depict significant distortion in the regional flow direction and locally few different flow directions were observed which can be attributed to some local factors like excessive pumping of groundwater. For instance, in the central city region near townhall (Supplementary Fig. 2), a prominent groundwater trough was observed where the water table elevation is lowered upto 128 m amsl. Field observations revealed that this area is marked by substantial human settlements which is heavily reliant on groundwater. Therefore, it can be deduced that the observed trough is likely a consequence of excessive groundwater pumping. Further, a groundwater mound was also observed near the confluence of Garrah and Khannaut

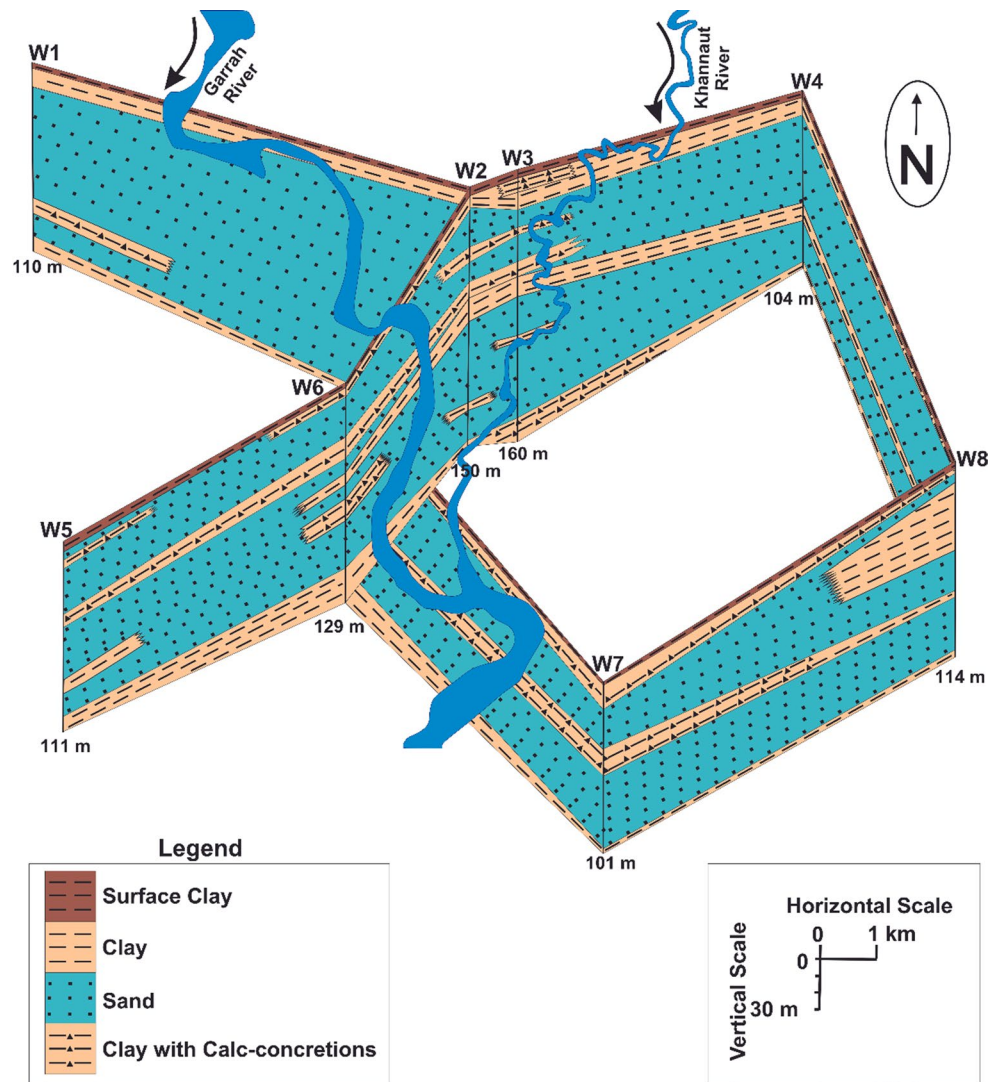
rivers in the southern peri-urban region from where the groundwater flows towards the two minor troughs of peri-urban region and a major trough of urban region (Supplementary Fig. 2). The contour pattern shows that both the rivers are contributing the aquifer system and hence are influent in nature.

The standardized analytical protocols recommended by APHA (1992) were employed to assess the physico-chemical parameters. The pH determination was done by a portable pH meter (Hach sensION), pre-calibrated with buffer solutions of known pH values (4, 7, and 10). Electrical conductivity (EC) and total dissolved solids (TDS) were measured with EC5 Portable Conductivity Meter (Hach sensION+), pre-calibrated using standards of 147 µS/cm, 1413 µS/cm, and 12.88 mS/cm. The determination of hardness (H) and calcium (Ca<sup>2+</sup>) involved a titration method utilizing ethylenediaminetetraacetic acid (EDTA); bicarbonate (HCO<sub>3</sub><sup>-</sup>) and chloride (Cl<sup>-</sup>) were analyzed through titration method using HCl and AgNO<sub>3</sub> respectively. Sodium (Na<sup>+</sup>) and potassium (K<sup>+</sup>) were estimated by flame emission photometry using Flame Photometer (SYSTRONICS 128). For determining sulphate (SO<sub>4</sub><sup>2-</sup>), gravimetric method was used while for nitrate (NO<sub>3</sub><sup>-</sup>), colorimetric method using phenol disulphonic acid was employed. The assessment of fluoride (F<sup>-</sup>) was carried out through spectrophotometer using SPADNS and ammonium molybdate spectrophotometric method was used for silica (SiO<sub>2</sub>) determination. Distilled water was used for preparing the solutions. Meticulous cleansing of the glassware with distilled water was carried out to avoid any contamination. For quality control and analytical accuracy of the data, the ionic balance error was computed as per Eq. 1. As per Hounslow (1995), the acceptable ionic balance error should be within ±10. The ionic charge balance error (CBE) fell within the acceptable limit, thus verifying the data accuracy.

$$CBE (\%) = \frac{\sum \text{Cation} - \sum \text{Anions}}{\sum \text{Cations} + \sum \text{Anions}} \times 100 \tag{1}$$

The one-way ANOVA statistical method was used to obtain a comprehensive insight into the seasonal fluctuations of the analyzed physico-chemical parameters. The data was tested at a 95% confidence level (α=0.05), with seasons and physico-chemical parameters being considered as independent and dependent variable respectively. The test aimed to ascertain whether there are significant differences in the measured datasets of individual parameters between two consecutive seasons at each monitoring site. If the p-value fall below 0.05, it implies significant seasonal variations among the analyzed parameters while p-value > 0.05 is an indicative of insignificant differences. It is crucial to highlight that, in the current study, monsoonal recharge was

**Fig. 3** Fence diagram of the study area



regarded as a predominant influencing factor for the seasonal variations. The pre-dominant hydrochemical facies were deciphered from the Piper Trilinear diagram. Gibbs diagram, diverse ionic relations, binary plots and chloralkaline indices were employed for delineating the mechanism regulating the groundwater chemical characteristics. Gibbs diagram is a scatter diagram proposed by Gibbs (1970) that have been widely employed to distinguish the effect of precipitation, rock-water interaction and evaporation process on chemical characteristics of groundwater. This plot was generated by correlating TDS and  $(Na)/(Na + Ca)$  for cations and TDS and  $(Cl)/(Cl + HCO_3)$  for anions. The role of silicate weathering was inferred using  $Na/Cl$  molal ratios and binary plots of  $Na + K$  vs. total cations and  $Ca + Mg$  vs.  $SO_4 + HCO_3$ . The impact of ion exchange process was deduced by evaluating chloralkaline indices i.e. CAI-1 (Eq. 2) and CAI-2 (Eq. 3) proposed by Schoeller (1967). The groundwater composition commonly gets altered as it percolates through the sub-surface. Such alterations are

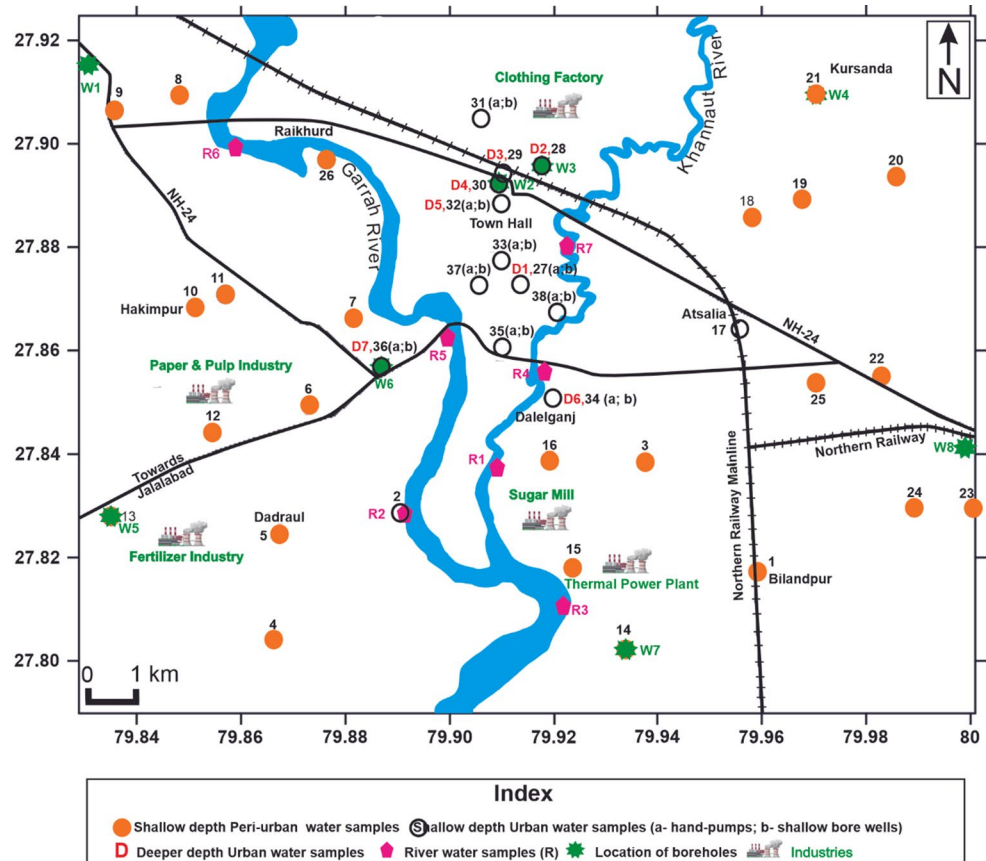
attributed to the process of ion exchange that is a phenomenon of adsorption/desorption. It is also referred to as base, or cation exchange due to the involvement of cations i.e.  $Na^+$ ,  $Ca^{2+}$  and  $Mg^{2+}$  (Todd and Mays 2005).

$$CAI - 1 = \frac{Na}{Na + K + Ca} \tag{2}$$

$$CAI - 2 = \frac{Cl}{Cl + HCO_3} \tag{3}$$

The influence of anthropogenic factors was assessed using Pearson correlation matrix. To assess the inter-relation between surface and groundwater, the river water and its nearby groundwater samples were compared for their major ion composition using Schoeller semi-logarithmic diagram. Silica values have been determined for estimating the temperature of sub-surface groundwater and its corresponding circulation depth as well as for understanding

**Fig. 4** Map depicting the river and groundwater sampling locations



the comparative influences of geogenic and anthropogenic factors on groundwater chemical characteristics. The groundwater appropriateness for its drinking requirement was examined by comparing the concentrations of physico-chemical parameters with drinking water quality standards set by BIS (2012) and WHO (2017) and by computing WQI. The WQI model is often used for the assessment of the drinking quality as it utilizes mathematical algorithms to transform existing water quality data into a singular numerical value. This approach offers an effective means of comprehending the overall quality of groundwater (Uddin et al. 2021, 2022; Singh et al. 2023). In the current study, 10 parameters have been used to compute WQI and for each water quality parameters, distinct weights ( $w_i$ ) were assigned depending upon its relative significance in governing the overall water quality. Equations 4–7 were employed in WQI calculations.

$$W_i = \frac{w_i}{\sum_{i=1}^n w_i} \tag{4}$$

$$Q_i = \frac{C_i - C_{ip}}{S_i - C_{ip}} \times 100 \tag{5}$$

$$S_{li} = W_i \times Q_i \tag{6}$$

$$WQI = \sum_{i=1}^n S_{li} \tag{7}$$

Where  $W_i$  = relative weight.

$w_i$  = weight assigned to individual parameter.

$n$  = no. of parameters.

$C_i$  = concentration of individual parameter in groundwater sample.

$C_{ip}$  = ideal value of the parameter in pure water ( $C_{ip} = 0$  for all, except pH,  $C_{ip} = 7$  for pH).

$S_i$  = desirable limit (DL) of individual parameter according to BIS 2012.

$S_{li}$  = sub-index of “ $i^{\text{th}}$ ” parameter.

$Q_i$  = rating given on the basis of “ $i^{\text{th}}$ ” parameter concentration.

To classify the water for irrigation purpose, Na concentration plays an important role as it interacts with the soil to reduce its permeability (Todd and Mays 2005). Therefore, the irrigational water quality was assessed by US Salinity Laboratory (USSL) plot, Kelley’s Ratio (KR) and Residual Sodium Carbonate (RSC). In USSL plot, SAR values (Eq. 8) which indicates the alkali hazard are plotted against EC which indicates salinity hazard (Richards 1954). KR (Eq. 9) also assess the adverse impact of Na on water quality intended for irrigation while RSC (Eq. 10) is extensively utilized for the prediction of additional Na hazard linked with

the precipitation of  $\text{CaCO}_3$  and  $\text{MgCO}_3$ . Water exhibiting KR values lower than 1 is suitable for irrigation (Karanth 1987). Water can be categorized as safe when RSC is below 1.25 meq/l, marginally suitable within the range of 1.25 to 2.5 meq/l while unsuitable when exceeding 2.5 meq/l.

$$\text{SAR} = \frac{\text{Na}}{\sqrt{\frac{\text{Ca} + \text{Mg}}{2}}} \quad (8)$$

$$\text{KR} = \frac{\text{Na}^+}{\text{Ca}^{2+} + \text{Mg}^{2+}} \quad (9)$$

$$\text{RSC} = (\text{CO}_3^{2-} + \text{HCO}_3^-) - (\text{Ca}^{2+} + \text{Mg}^{2+}) \quad (10)$$

The industrial equipment often develops scaling or get corroded because of adverse reactions occurring at high pressure and temperature (Amiri et al. 2021). These reactions may enhance the micro-organisms biological activity and can reduce the power and nominal life of the water transmission network (Vasconcelos et al. 2015). Thus, the corrosive and scaling tendencies of water for their use in industrial equipment was evaluated using Larson-Skold Index (L-SI) as per Eq. 11. L-SI values less than 0.8 indicates that  $\text{Cl}^-$  and  $\text{SO}_4^{2-}$  do not interfere in scale formation and will be non-corrosive; between 0.8 and 1.2 indicates that they may interfere and may cause corrosion and greater than 1.2 indicate their interference in scale formation and will be highly corrosive.

$$\text{L-SI} = \frac{\text{SO}_4^{2-} + \text{Cl}^-}{\text{HCO}_3^- + \text{CO}_3^{2-}} \quad (11)$$

## Results and discussion

### Hydrochemical characteristics

The ranges and mean values of physico-chemical parameters for all type of water samples are summarized in Table 2 and detailed location wise data has been provided in Supplementary Table 1 for PRMS, 2019 and Supplementary Table 2 for POMS, 2019. In case of peri-urban shallow samples, the mean pH values are 8.04 and 7.93 in PRMS, 2019 and POMS, 2019 respectively. For urban shallow samples, it is 7.88 in both the sampling periods while for urban deep samples, it is 7.91 and 8.23 in PRMS, 2019 and POMS, 2019 respectively. The pH values revealed the alkaline nature of groundwater in both the sampling periods. The mean electrical conductivity (EC) values are 830  $\mu\text{S}/\text{cm}$  for peri-urban shallow, 1285  $\mu\text{S}/\text{cm}$  for urban shallow and 756  $\mu\text{S}/\text{cm}$

for urban deep samples in PRMS, 2019 while in POMS, 2019, it is 853  $\mu\text{S}/\text{cm}$  for peri-urban shallow, 1344  $\mu\text{S}/\text{cm}$  for urban shallow and 815  $\mu\text{S}/\text{cm}$  for urban deep samples. The mean TDS values were 539 for peri-urban shallow samples, 832 for urban shallow samples and 491 mg/l for urban deep samples in PRMS, 2019 while in POMS, 2019, it is 556 mg/l for peri-urban shallow samples, 873 mg/l for urban shallow and 534 mg/l for urban deep samples. Relatively high TDS concentrations in urban shallow samples might be attributed to sewage, urban runoff and industrial wastewater. The mean values of the major cations as well as anions were compared to infer their order of abundance. The most prevalent cation was  $\text{Na}^+$  followed by  $\text{Ca}^{2+}$ ,  $\text{Mg}^{2+}$  and  $\text{K}^+$  and anion was  $\text{HCO}_3^-$  followed by  $\text{Cl}^-$ ,  $\text{SO}_4^{2-}$ ,  $\text{NO}_3^-$  and  $\text{F}^-$ . The seasonal fluctuations in the physico-chemical parameters was assessed by one-way ANOVA statistical approach (Table 3). For peri-urban shallow samples, pH,  $\text{K}^+$ ,  $\text{Na}^+$  and  $\text{Cl}^-$  ( $p < 0.05$ ) show significant seasonal variations with p values less than 0.05 indicating the monsoonal recharge influence on these parameters. However, the remaining parameters showed  $p > 0.05$ , thereby signifying that there were no discernible seasonal fluctuations. In case of urban shallow and deep samples, most of the parameters show insignificant seasonal variations ( $p > 0.05$ ), indicating they have remained relatively constant throughout the seasons. The prevalence of impervious cover like asphalt roads, settlements, concrete or paved surfaces in the urban region might have resulted in reduced rate of rainfall recharge and consequently lesser dilution effect. River samples revealed notable seasonal variations ( $p < 0.05$ ) in EC, TDS,  $\text{Cl}^-$ ,  $\text{K}^+$  and  $\text{SO}_4^{2-}$  suggesting the strong influence of monsoonal recharge.

The *Piper Trilinear* plots of groundwater samples for PRMS, 2019 and POMS, 2019 (Fig. 5a and b) revealed that by and large  $\text{Ca} + \text{Mg} - \text{HCO}_3$  is the pre-dominant hydrochemical facies identified for most of the groundwater samples, suggesting that groundwater genesis is majorly of bicarbonate ( $\text{HCO}_3$ ) type, thereby acquiring temporary hardness. Few urban shallow samples also lie in the mixed zone suggesting the absence of a dominant cation-anion composition. The predominant facies identified for river water samples was also  $\text{Ca} + \text{Mg} - \text{HCO}_3$ .

### Processes governing the groundwater chemistry

The *Gibbs plots* for PRMS, 2019 (Fig. 6a-b) and POMS, 2019 (Fig. 6c-d) revealed that maximum groundwater samples fell under rock dominance field, thereby, revealing that water-rock interaction is the prime mechanism that regulates the groundwater chemical characteristics. However,  $\text{Na}^+$  exhibit a wide distribution in both sampling periods, thereby suggesting that it might have been originated from



**Table 2** Range and mean values of physico-chemical parameters during PRMS and POMS, 2019

| Physico-chemical parameters   | WHO (2017) Standards |      |    | BIS (2012) Standards |      |    | Peri-urban shallow samples |       |      | Urban shallow samples |      |      | Urban deep samples |      |      | River water samples |      |      |
|-------------------------------|----------------------|------|----|----------------------|------|----|----------------------------|-------|------|-----------------------|------|------|--------------------|------|------|---------------------|------|------|
|                               | DL                   | PL   | NR | DL                   | PL   | NR | Min                        | Max   | Mean | Min                   | Max  | Mean | Min                | Max  | Mean | Min                 | Max  | Mean |
| pH                            | 7                    | 8.5  | -  | 6.5-8.5              | NR   | -  | 7.51                       | 8.24  | 8.04 | 7.13                  | 8.22 | 7.88 | 7.08               | 8.13 | 7.91 | 7.85                | 8.09 | 7.93 |
| EC                            | -                    | -    | -  | -                    | -    | -  | 656                        | 1110  | 830  | 663                   | 1832 | 1285 | 706                | 891  | 756  | 526                 | 648  | 589  |
| TDS                           | 500                  | 1500 | -  | 500                  | 2000 | -  | 440                        | 704   | 539  | 432                   | 1146 | 832  | 461                | 578  | 491  | 361                 | 417  | 386  |
| Hardness                      | 100                  | 500  | -  | 200                  | 600  | -  | 140                        | 384   | 210  | 164                   | 388  | 311  | 152                | 208  | 177  | 120                 | 152  | 141  |
| Ca <sup>2+</sup>              | 75                   | 200  | -  | 75                   | 200  | -  | 19                         | 67    | 45   | 22                    | 101  | 54   | 26                 | 38   | 33   | 32                  | 42   | 36   |
| Mg <sup>2+</sup>              | 30                   | 150  | -  | 30                   | 100  | -  | 8                          | 59    | 24   | 19                    | 66   | 43   | 19                 | 30   | 23   | 8                   | 18   | 13   |
| Na <sup>+</sup>               | -                    | -    | -  | -                    | -    | -  | 16                         | 76    | 41   | 56                    | 148  | 93   | 44                 | 72   | 54   | 24                  | 32   | 27   |
| K <sup>+</sup>                | -                    | -    | -  | -                    | -    | -  | 4                          | 13    | 7    | 6                     | 42   | 23   | 6                  | 8    | 7    | 4                   | 8    | 6    |
| Cl <sup>-</sup>               | 200                  | 600  | -  | 250                  | 1000 | -  | 14                         | 80    | 36   | 48                    | 165  | 93   | 34                 | 68   | 54   | 14                  | 31   | 22   |
| SO <sub>4</sub> <sup>2-</sup> | 200                  | 400  | -  | 200                  | 400  | -  | 11                         | 81    | 27   | 38                    | 150  | 79   | 18                 | 51   | 33   | 18                  | 21   | 20   |
| HCO <sub>3</sub> <sup>-</sup> | -                    | -    | -  | 200                  | 600  | -  | 208                        | 455   | 295  | 208                   | 533  | 372  | 234                | 299  | 267  | 156                 | 221  | 189  |
| NO <sub>3</sub> <sup>-</sup>  | 45                   | NR   | -  | 45                   | NR   | -  | 0                          | 13.08 | 1.27 | 0                     | 77.4 | 43.8 | 0                  | 4.61 | 0.83 | 0.79                | 8.06 | 4.69 |
| F <sup>-</sup>                | 1                    | 1.5  | -  | 1                    | 1.5  | -  | 0                          | 0.57  | 0.21 | 0                     | 0.88 | 0.24 | 0                  | 0.39 | 0.11 | 0                   | 0.39 | 0.13 |
| SiO <sub>2</sub>              | -                    | -    | -  | -                    | -    | -  | 30                         | 50    | 37   | 30                    | 45   | 37   | 52                 | 63   | 58   | 26                  | 32   | 29   |
| <b>POMS, 2019</b>             |                      |      |    |                      |      |    |                            |       |      |                       |      |      |                    |      |      |                     |      |      |
| Physico-chemical parameters   | WHO (2017) Standards |      |    | BIS (2012) Standards |      |    | Peri-urban shallow samples |       |      | Urban shallow samples |      |      | Urban deep samples |      |      | River water samples |      |      |
|                               | DL                   | PL   | NR | DL                   | PL   | NR | Min                        | Max   | Mean | Min                   | Max  | Mean | Min                | Max  | Mean | Min                 | Max  | Mean |
| pH                            | 7                    | 8.5  | -  | 6.5-8.5              | NR   | -  | 7.67                       | 8.24  | 7.93 | 7.58                  | 8.30 | 7.88 | 8.14               | 8.35 | 8.23 | 7.88                | 8.39 | 8.07 |
| EC                            | -                    | -    | -  | -                    | -    | -  | 642                        | 1076  | 853  | 907                   | 1765 | 1344 | 656                | 933  | 815  | 587                 | 783  | 685  |
| TDS                           | 500                  | 1500 | -  | 500                  | 2000 | -  | 424                        | 680   | 556  | 603                   | 1128 | 873  | 433                | 601  | 534  | 385                 | 509  | 451  |
| Hardness                      | 100                  | 500  | -  | 200                  | 600  | -  | 148                        | 304   | 213  | 168                   | 436  | 320  | 172                | 220  | 194  | 120                 | 164  | 142  |
| Ca <sup>2+</sup>              | 75                   | 200  | -  | 75                   | 200  | -  | 30                         | 66    | 50   | 30                    | 83   | 60   | 32                 | 42   | 37   | 30                  | 43   | 37   |
| Mg <sup>2+</sup>              | 30                   | 150  | -  | 30                   | 100  | -  | 9                          | 43    | 22   | 22                    | 58   | 42   | 19                 | 28   | 25   | 10                  | 15   | 12   |
| Na <sup>+</sup>               | -                    | -    | -  | -                    | -    | -  | 20                         | 88    | 51   | 84                    | 128  | 104  | 48                 | 72   | 60   | 24                  | 52   | 36   |
| K <sup>+</sup>                | -                    | -    | -  | -                    | -    | -  | 4                          | 16    | 9    | 9                     | 38   | 24   | 9                  | 12   | 10   | 6                   | 16   | 9    |
| Cl <sup>-</sup>               | 200                  | 600  | -  | 250                  | 1000 | -  | 23                         | 77    | 44   | 62                    | 153  | 97   | 48                 | 85   | 61   | 26                  | 51   | 37   |
| SO <sub>4</sub> <sup>2-</sup> | 200                  | 400  | -  | 200                  | 400  | -  | 12                         | 76    | 29   | 59                    | 143  | 87   | 19                 | 73   | 33   | 18                  | 27   | 23   |
| HCO <sub>3</sub> <sup>-</sup> | -                    | -    | -  | 200                  | 600  | -  | 234                        | 403   | 310  | 247                   | 546  | 397  | 260                | 325  | 295  | 156                 | 234  | 202  |
| NO <sub>3</sub> <sup>-</sup>  | 45                   | NR   | -  | 45                   | NR   | -  | 0                          | 14.70 | 2.24 | 0                     | 99.9 | 51.5 | 0                  | 3.19 | 1.59 | 1.15                | 13.6 | 7.01 |
| F <sup>-</sup>                | 1                    | 1.5  | -  | 1                    | 1.5  | -  | 0                          | 0.51  | 0.14 | 0                     | 0.88 | 0.19 | 0                  | 0.44 | 0.18 | 0                   | 0.56 | 0.16 |
| SiO <sub>2</sub>              | -                    | -    | -  | -                    | -    | -  | 30                         | 48    | 36.7 | 33                    | 44   | 39   | 51                 | 63   | 57   | 30                  | 32   | 30   |

**Note:** All values are in mg/l except pH and EC (µS/cm), DL- desirable limit, PL- Permissible limit, NR- No relaxation

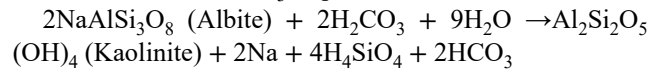
**Table 3** Comparative analysis of physico-chemical parameters through one-way ANOVA for PRMS and POMS, 2019

| Parameters                    | p- values                  |                       |                    |                     |
|-------------------------------|----------------------------|-----------------------|--------------------|---------------------|
|                               | Peri-urban shallow samples | Urban shallow samples | Urban deep samples | River water samples |
| pH                            | 0.03                       | 0.86                  | 0.0012             | 0.139               |
| EC                            | 0.49                       | 0.61                  | 0.101              | 0.012               |
| TDS                           | 0.408                      | 0.54                  | 0.07               | 0.01                |
| H                             | 0.86                       | 0.71                  | 0.17               | 0.88                |
| Ca <sup>2+</sup>              | 0.16                       | 0.49                  | 0.139              | 0.655               |
| Mg <sup>2+</sup>              | 0.47                       | 0.84                  | 0.4                | 0.929               |
| Na <sup>+</sup>               | 0.04                       | 0.14                  | 0.125              | 0.072               |
| K <sup>+</sup>                | 0.002                      | 0.63                  | 7.8E-05            | 0.023               |
| Cl <sup>-</sup>               | 0.03                       | 0.68                  | 0.26               | 0.004               |
| SO <sub>4</sub> <sup>2-</sup> | 0.7                        | 0.432                 | 0.99               | 0.026               |
| HCO <sub>3</sub> <sup>-</sup> | 0.3                        | 0.432                 | 0.079              | 0.421               |
| NO <sub>3</sub> <sup>-</sup>  | 0.06                       | 0.45                  | 0.329              | 0.29                |
| F <sup>-</sup>                | 0.1408                     | 0.5                   | 0.3                | 0.704               |
| SiO <sub>2</sub>              | 0.63                       | 0.09                  | 0.66               | 0.144               |

Note Significance level is 0.05

diverse sources (Bai et al. 2022). Overall, it was found that rock-water interaction is majorly governing the chemical characteristics of majority of the samples. In alluvial plains, many researchers have found that the prime mechanism impacting groundwater chemistry is the interaction between rock and water (Raju et al. 2011; Madhav et al. 2018). Also, the samples falling outside the three designated fields pinpoints towards the impact of anthropogenic influences on groundwater chemistry (Annapoorna and Janardhana 2015).

The role of *silicate weathering* was inferred using Na/Cl molal ratios. A ratio of equal to or below 1 signifies the release of Na from halite dissolution whereas if it is more than 1, silicate weathering is considered to be the prime contributor of Na. Also, if the source of Na is silicate weathering, then groundwater must show the predominance of HCO<sub>3</sub> (Okiongbo and Akpofure 2014). This is because the feldspar minerals react with carbonic acid in the presence of water and liberates HCO<sub>3</sub> as per the reaction



The Na/Cl binary plots for PRMS, 2019 (Fig. 7a) and POMS, 2019 (Fig. 7b) depicts Na/Cl ratio more than 1. Also, HCO<sub>3</sub> was the predominant anion in the groundwater. This infers that weathering of silicates is influencing the groundwater chemistry. The results can further be validated by Na + K vs. total cations as well as Ca + Mg vs. SO<sub>4</sub> + HCO<sub>3</sub> bivariate plots, where most of the samples fall below 1:1 equiline in both plots, thereby, reflecting that the groundwater chemistry is regulated by weathering of silicates (Rajmohan and Elango 2004). Further, Na + K vs. total cations for PRMS, 2019 and POMS, 2019 (Fig. 7c and d respectively) shows that all types of groundwater samples lie below equiline. This reaffirms that silicate weathering is influencing the groundwater chemistry. Further, Ca + Mg vs. SO<sub>4</sub> + HCO<sub>3</sub> plot depicts that maximum number of groundwater samples falls below the equiline in PRMS, 2019 and POMS, 2019 (Fig. 7e and f respectively). It further confirms

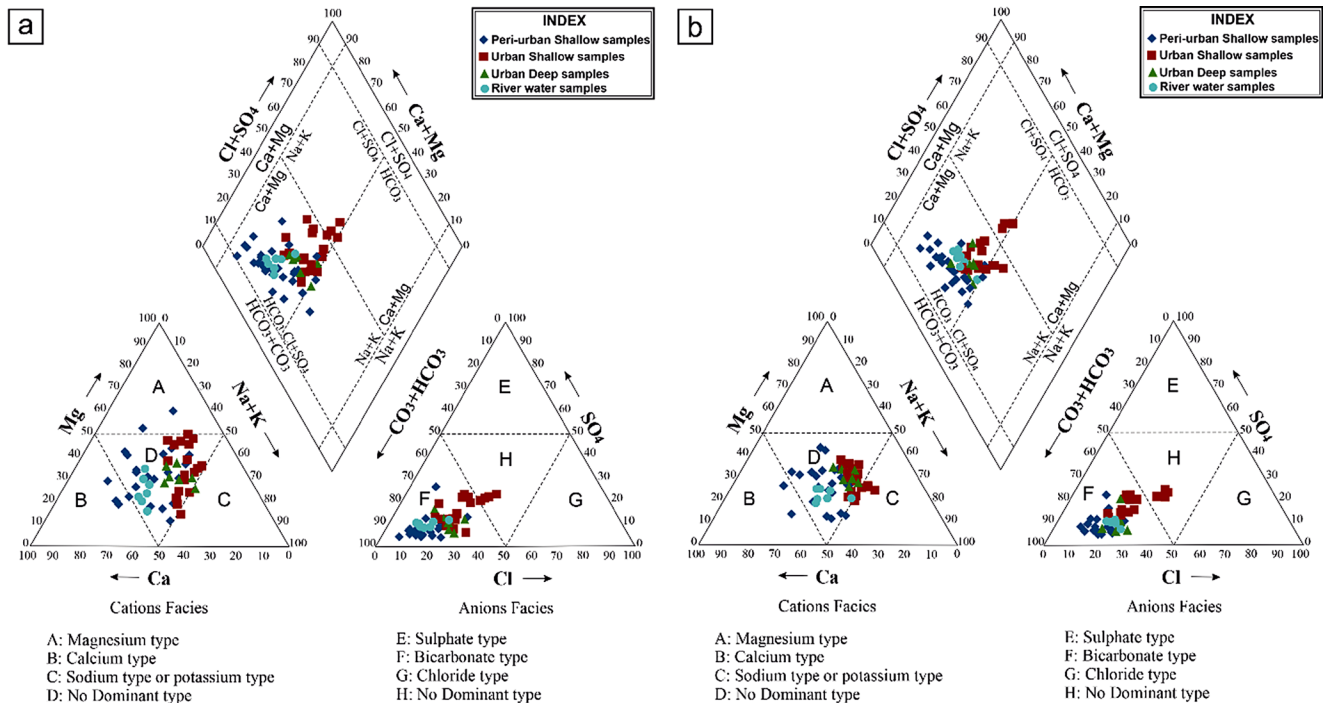


**Fig. 5** Piper trilinear plots (a) PRMS, 2019, (b) POMS, 2019

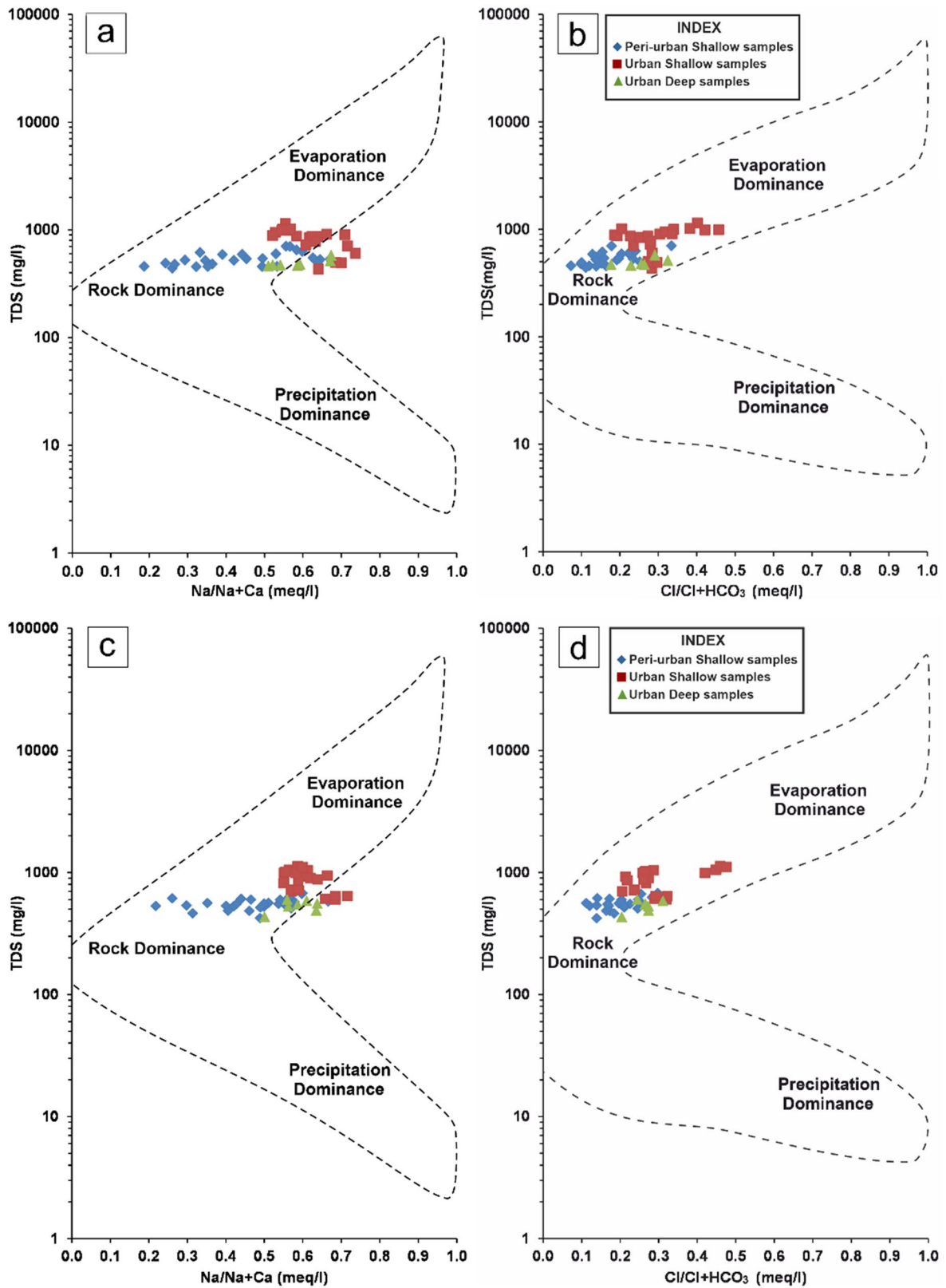


Fig. 6 Gibbs plots for (a-b) PRMS, 2019, (c-d) POMS, 2019

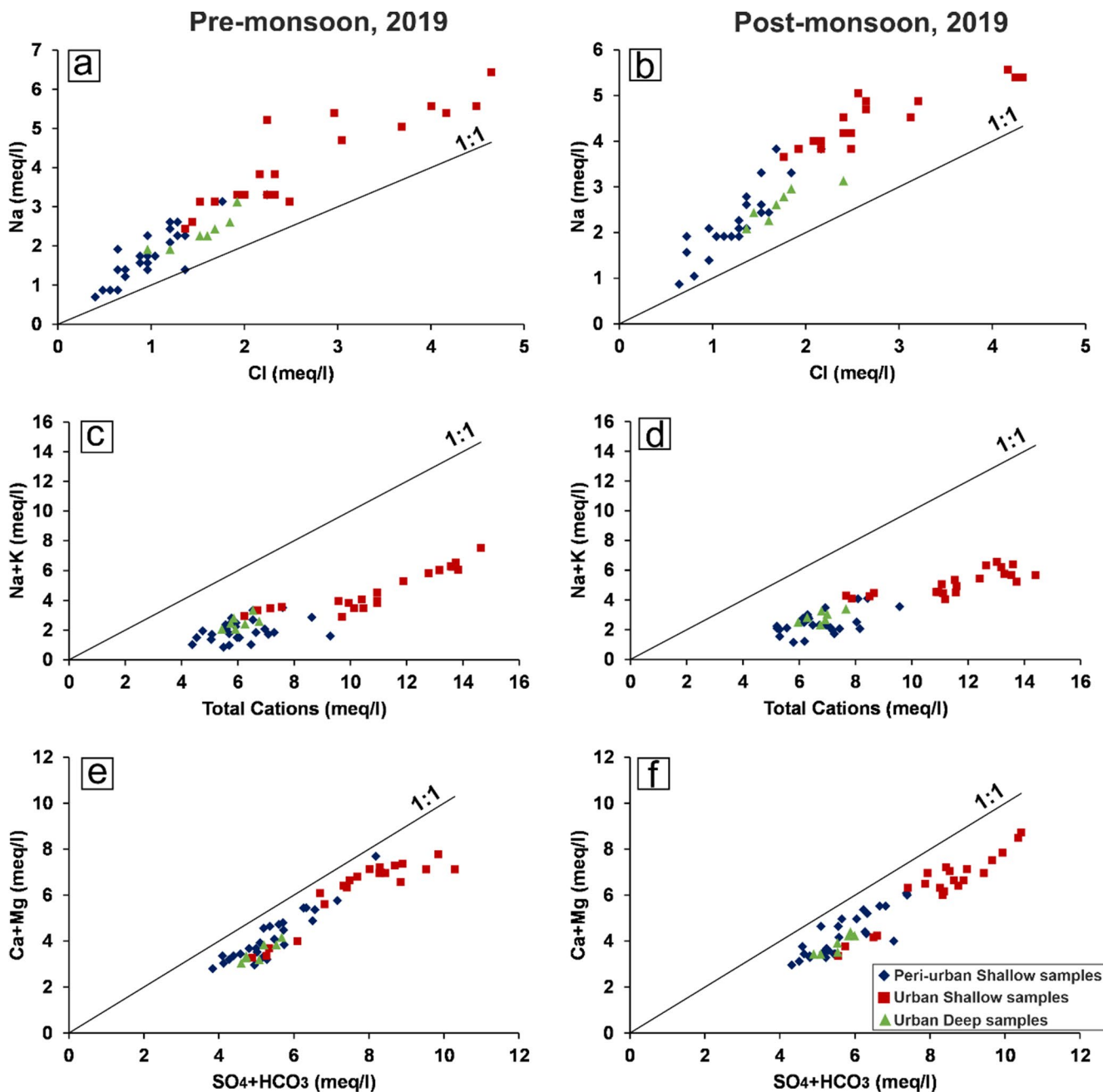


Fig. 7 Scatter plots (a-b) Na vs. Cl, (c-d) Na + K vs. total cations, (e-f) Ca + Mg vs. SO<sub>4</sub> + HCO<sub>3</sub>

that weathering of silicate is one of the major processes in acquisition of major ions.

The role of *ion exchange process* in influencing the groundwater chemistry was inferred by evaluating chloralkaline indices i.e. CAI-1 and CAI-2. Clay minerals owing to their negatively charged surface acts as an efficient ion exchanger. As a result, cations in the groundwater easily gets exchanged. The direct ion exchange is the mechanism wherein Na<sup>+</sup>/K<sup>+</sup> in groundwater undergoes an exchange with Ca<sup>2+</sup>/Mg<sup>2+</sup> in rock. Consequently, the concentration

of Na<sup>+</sup> or K<sup>+</sup> in the water decreases, resulting in positive chloralkaline indices. On the contrary, reverse ion exchange process results in negative indices (Li et al. 2018). Both the ratios for all types of samples were found to be negative in both the sampling periods, thus depicting the type of cation exchange (Supplementary Tables 1 and 2). Further, if cation exchange influences the composition of groundwater, then there occurs a linear relation between Na-Cl and Ca + Mg-HCO<sub>3</sub>-SO<sub>4</sub> with slope of -1 (Fisher and Mullican 1997). The plots for PRMS, 2019 (Fig. 8a) and POMS, 2019

**Fig. 8** Scatter plots of Na-Cl and Ca + Mg-HCO<sub>3</sub>-SO<sub>4</sub> for (a) PRMS, 2019 (b) POMS, 2019

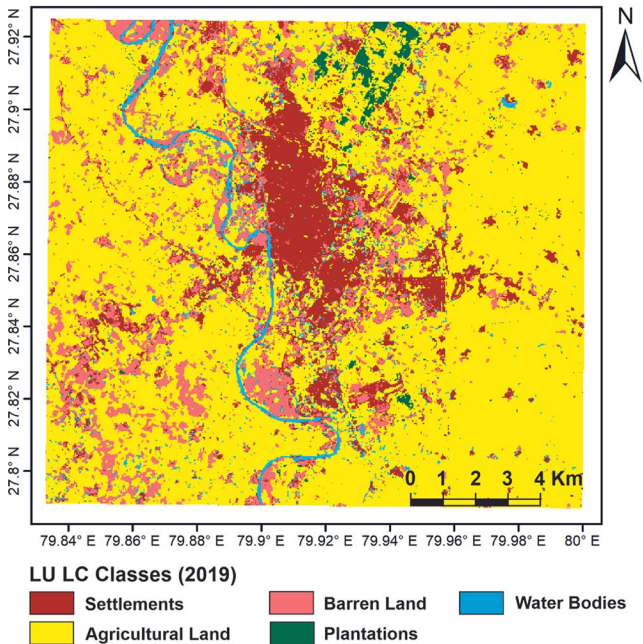
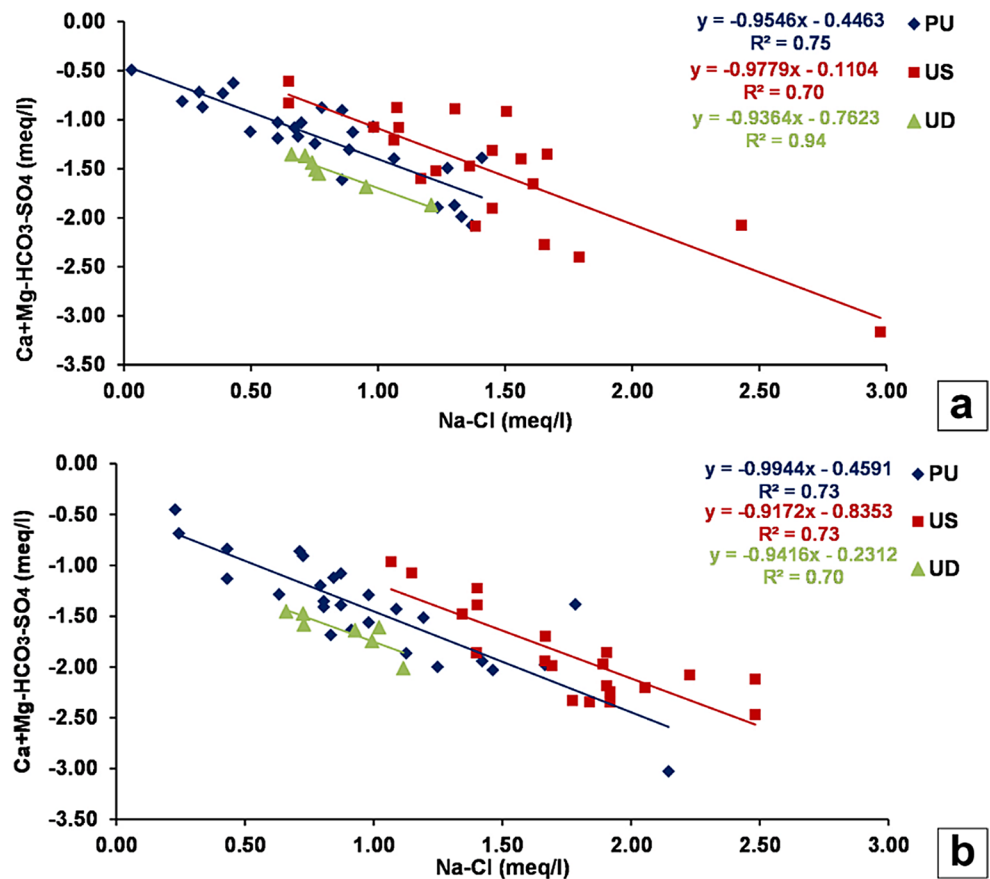


**Fig. 9** Land use land cover map

(Fig. 8b) show that for all the samples, there occurs a linear relationship between the above parameters with a slope varying from -0.9 to -1. This confirms that cation exchange is also one of the process that is influencing the groundwater chemistry.

The *anthropogenic factors*, along with geogenic processes, frequently impact the groundwater quality. Given the intricate connection between groundwater and Land Use-Land Cover (LU-LC) patterns, gaining an understanding of the LU-LC pattern of the area is crucial for comprehending the human induced impact on groundwater quality. Additionally, the sources of groundwater contamination also differ depending on the specific land uses. For instance, in urban areas, the major sources of groundwater contamination are mainly sewage effluents, domestic wastes water etc. while peri-urban areas might experience more agricultural pollution due to excessive use of pesticides and fertilizers. Therefore, the LU-LC map of the study for the year 2019 was generated by using LANDSAT image (<http://earthexplorer.usgs.gov>) having a spectral resolution of 30 m to differentiate the peri-urban and urban regions. As mentioned earlier and is evident from the LU-LC map (Fig. 9), the central region is extensively urbanized and classified as an urban area, while the peripheral fringe areas are designated as peri-urban regions, therefore, the influence

of anthropogenic activities on groundwater quality was assessed in both these regions by correlating the concentration of TDS with  $\text{Cl}^-$ ,  $\text{SO}_4^{2-}$  and  $\text{NO}_3^-$  using Pearson correlation matrix (Table 4). As anthropogenic activities often cause variations in TDS of groundwater and  $\text{Cl}^-$ ,  $\text{SO}_4^{2-}$  and  $\text{NO}_3^-$  are among the major ions that can be derived from anthropogenic sources, consequently, correlating these ions with TDS becomes a means to deduce the human induced impacts on groundwater quality (Marghade et al. 2011; Wali et al. 2019).

For peri-urban shallow samples, TDS and  $\text{Cl}^-$  depicts a strong positive correlation of 0.8 in PRMS, 2019 and moderate correlation of 0.6 in POMS, 2019, thereby, revealing similar source of origin. Irrigation water might be a significant anthropogenic source of  $\text{Cl}^-$  in groundwater of peri-urban region. However, TDS do not depict any significant correlation with  $\text{SO}_4^{2-}$  and  $\text{NO}_3^-$ , in both the sampling periods, thereby, pinpointing towards distinct sources of origin.

For urban shallow samples, TDS depicts a moderate positive correlation of 0.7 with  $\text{Cl}^-$ , 0.6 with  $\text{SO}_4^{2-}$  and 0.7 with  $\text{NO}_3^-$  in PRMS, 2019. In POMS, 2019 also, there is a moderate positive correlation of TDS with  $\text{Cl}^-$  (0.7),  $\text{SO}_4^{2-}$  (0.7) and  $\text{NO}_3^-$  (0.6), thus, signifying that they might have been originating from similar sources. The major anthropogenic sources of these ions in urban environment can be domestic wastewater, sewage effluents, septic tank leakages etc.

For urban deep samples, TDS shows a moderate correlation of 0.7 with  $\text{Cl}^-$  in PRMS, 2019 and 0.5 in POMS, 2019, thereby, revealing their similar source of origin. An insignificant correlation of TDS with  $\text{SO}_4^{2-}$  and  $\text{NO}_3^-$  in

both the sampling periods indicates their origin from different sources.

The *groundwater-surface water interaction* was assessed by comparing the major ion composition of river water and its nearby groundwater samples using Schoeller semi-logarithmic diagram in PRMS, 2019 (Fig. 10a–g) and POMS, 2019 (Fig. 11a–g). The major ion concentrations of all water samples for both sampling periods is given in Supplementary Table 3. A similar trend was observed in the concentrations of  $\text{K}^+$ ,  $\text{Cl}^-$ ,  $\text{SO}_4^{2-}$  and  $\text{HCO}_3^-$  ions for Garrah river samples and its nearby groundwater samples in PRMS, 2019 (Fig. 10a, c and e) and POMS, 2019 (Fig. 11a, c and e). Whenever there is a rise or fall in the concentration of these ions in river water, a corresponding fluctuation in the concentration of the same ions in groundwater occurs, albeit with a slightly varying magnitude. Khannaut river samples and its nearby groundwater samples also depicts a similar trend in the concentrations of  $\text{K}^+$ ,  $\text{Cl}^-$ ,  $\text{SO}_4^{2-}$  and  $\text{HCO}_3^-$  ions in, PRMS, 2019 (Fig. 10b, d and f) and POMS, 2019 (Fig. 11b, d and f). However, the magnitude difference between the upper (R7) and middle (R4) reaches of Khannaut river and groundwater samples is much pronounced (Figs. 10b and d and 11b and d). The concentrations of all the ions are more in groundwater samples as compared to river water samples. These two samples are quite close to the city area; thus, anthropogenic inputs might have resulted in elevated concentrations of  $\text{SO}_4^{2-}$  and  $\text{Cl}^-$  in groundwater. For  $\text{Ca}^{2+}$ ,  $\text{Mg}^{2+}$  and  $\text{Na}^+$ , no marked trend was noticed between the river and groundwater samples, which implies the role of some other processes rather than surface and groundwater interaction in acquisition of these ions. The

**Table 4** Pearson correlation matrix of all types of groundwater samples

| Peri-urban shallow samples |      |               |                    |                 | POMS, 2019    |      |               |                    |                 |
|----------------------------|------|---------------|--------------------|-----------------|---------------|------|---------------|--------------------|-----------------|
| PRMS, 2019                 |      |               |                    |                 | POMS, 2019    |      |               |                    |                 |
| Parameters                 | TDS  | $\text{Cl}^-$ | $\text{SO}_4^{2-}$ | $\text{NO}_3^-$ | Parameters    | TDS  | $\text{Cl}^-$ | $\text{SO}_4^{2-}$ | $\text{NO}_3^-$ |
| TDS                        | 1    |               |                    |                 | TDS           | 1    |               |                    |                 |
| Cl                         | 0.8  | 1             |                    |                 | Cl            | 0.6  | 1             |                    |                 |
| $\text{SO}_4$              | 0.5  | 0.3           | 1                  |                 | $\text{SO}_4$ | 0.3  | 0             | 1                  |                 |
| $\text{NO}_3$              | -0.2 | -0.2          | -0.2               | 1               | $\text{NO}_3$ | -0.3 | -0.1          | -0.3               | 1               |
| Urban shallow samples      |      |               |                    |                 | POMS, 2019    |      |               |                    |                 |
| PRMS, 2019                 |      |               |                    |                 | POMS, 2019    |      |               |                    |                 |
| Parameters                 | TDS  | $\text{Cl}^-$ | $\text{SO}_4^{2-}$ | $\text{NO}_3^-$ | Parameters    | TDS  | $\text{Cl}^-$ | $\text{SO}_4^{2-}$ | $\text{NO}_3^-$ |
| TDS                        | 1    |               |                    |                 | TDS           | 1    |               |                    |                 |
| Cl                         | 0.7  | 1             |                    |                 | Cl            | 0.7  | 1             |                    |                 |
| $\text{SO}_4$              | 0.6  | 0.6           | 1                  |                 | $\text{SO}_4$ | 0.7  | 0.7           | 1                  |                 |
| $\text{NO}_3$              | 0.7  | 0.5           | 0.3                | 1               | $\text{NO}_3$ | 0.6  | 0.5           | 0.4                | 1               |
| Urban deep samples         |      |               |                    |                 | POMS, 2019    |      |               |                    |                 |
| PRMS, 2019                 |      |               |                    |                 | POMS, 2019    |      |               |                    |                 |
| Parameters                 | TDS  | $\text{Cl}^-$ | $\text{SO}_4^{2-}$ | $\text{NO}_3^-$ | Parameters    | TDS  | $\text{Cl}^-$ | $\text{SO}_4^{2-}$ | $\text{NO}_3^-$ |
| TDS                        | 1    |               |                    |                 | TDS           | 1    |               |                    |                 |
| Cl                         | 0.7  | 1             |                    |                 | Cl            | 0.5  | 1             |                    |                 |
| $\text{SO}_4$              | -0.5 | -0.6          | 1                  |                 | $\text{SO}_4$ | 0.3  | -0.4          | 1                  |                 |
| $\text{NO}_3$              | -0.3 | -0.1          | 0.2                | 1               | $\text{NO}_3$ | 0.3  | -0.5          | 0.5                | 1               |

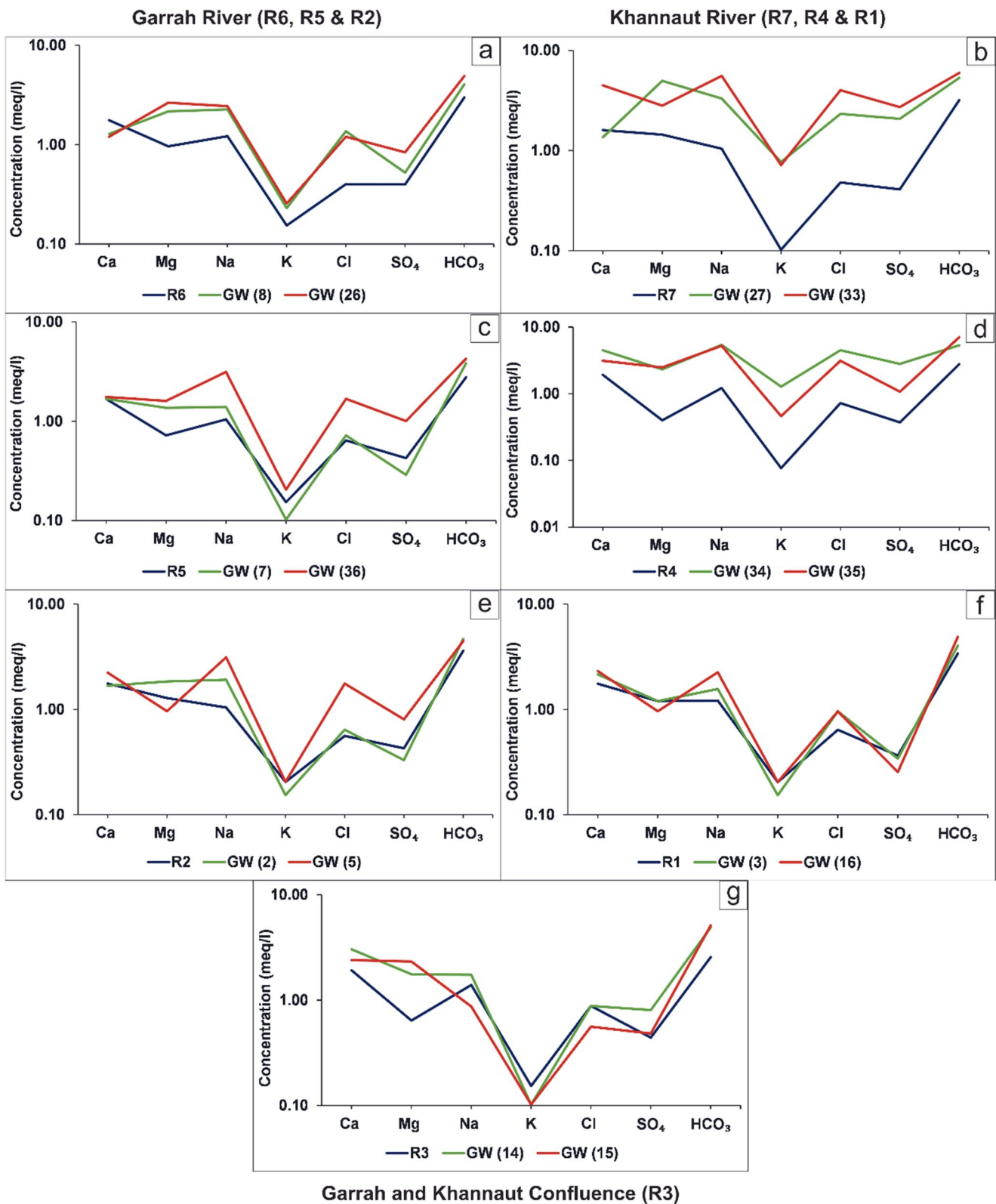


Fig. 10 Schoeller diagrams depicting trends in major ion composition of river water and its nearby groundwater samples for PRMS, 2019

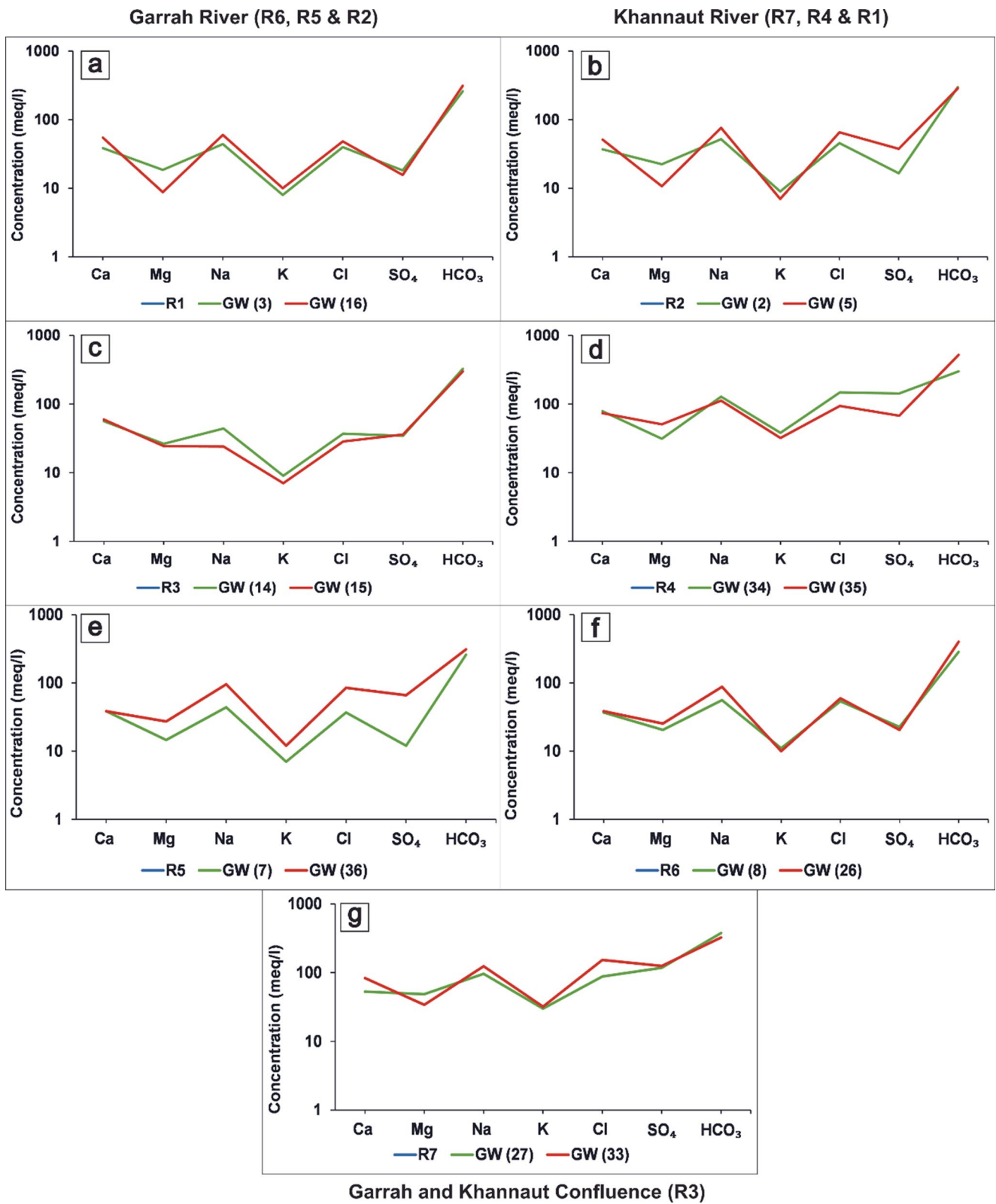


Fig. 11 Schoeller diagrams depicting trends in major ion composition of river water and its nearby groundwater samples for POMS, 2019



chemistry of the confluence river water sample and groundwater sample is also quite similar in both the sampling periods (Figs. 10g and 11g). Further, dominant groundwater facies inferred using Piper Trilinear diagram for both river and groundwater samples is Ca + Mg-HCO<sub>3</sub> (Fig. 5a and b). Similar variation in the concentration of most of the ions (K<sup>+</sup>, Cl<sup>-</sup>, SO<sub>4</sub><sup>2-</sup> and HCO<sub>3</sub><sup>-</sup>) reveals similarity in groundwater and river water characteristics. Thus, it can be inferred that surface water might be interacting with groundwater. This can also be validated from the water table contour map which revealed the influent nature of the rivers (Supplementary Fig. 2). However, dissimilar trend in the concentrations of Ca<sup>2+</sup>, Mg<sup>2+</sup> and Na<sup>+</sup> pinpoints toward processes other than surface and groundwater interaction in influencing the groundwater chemistry.

### Silica implications

The circulating groundwater acquires silica, when it gets released from breakdown of the silicate minerals by chemical weathering. Thus, water-rock interaction is the exclusive and unequivocal source of SiO<sub>2</sub> in groundwater (Hem 1985). The groundwater silica content rises because of their contact with silicate rocks for a longer time period. Also, water coming from deeper depths generally shows higher silica content as compared to the one descending from shallow depth (Marchand et al. 2002). Thus, groundwater with relatively higher silica content indicates strong rock-water interaction. The median worldwide SiO<sub>2</sub> concentration in groundwater can be around 17 mg/l, but this value could vary, potentially reaching levels of 70–80 mg/l depending upon different factors viz. pH, lithology of the aquifer, temperature etc. (Saba 2016). Additionally, the silica solubility in groundwater varies directly with temperature (Fournier and Potter 1982). The values of silica converted to aquifer

temperature also indicate to what depth the groundwater descends, if the normal geothermal gradient is assumed to be of 30 °C/km. Swanberg and Morgan (1978) pioneered the use of silica geothermometry in groundwater systems, showcasing its effectiveness through a comprehensive investigation of more than 70,000 groundwater samples across the United States. Prior investigations utilizing silica geothermometry have also been conducted in regions of the Ganga plain (Khan and Umar 2010; Khan et al. 2015b).

For determining the sub-surface temperatures by silica values of natural water that is in equilibrium with either chalcedony or quartz, several silica geothermometric equations were proposed through time. Various geothermometers are valid within distinct temperature ranges due to their diverse equilibration rates and distinct responses to cooling in upflow zones. The quartz geothermometer is usually employed in systems with high temperature whereas in low temperature systems, chalcedony geothermometer is used. The one that is considered relatively appropriate for groundwater systems considers the solubility of chalcedony and is proposed by Fournier and Potter 1982 (Eq. 12).

$$t^{\circ}\text{C} = \left( \frac{1032}{4.69 - \log\text{SiO}_2} \right) - 273.15 \quad (12)$$

where,

$t^{\circ}\text{C}$  = chalcedony derived groundwater temperature.

Substituting the calculated values of silica in Eq. 12, the groundwater chalcedony temperature was estimated. However, the estimated temperature has to be corrected for ambient air temperature during the sampling seasons. For instance, during POMS, 2019, the ambient air temperature of the study area was around 27°C and the estimated chalcedony temperature was 48°C. When this estimated temperature was corrected for the ambient air temperature, then it signifies a temperature of around 21°C over and above an average temperature of air, that in turn indicates that groundwater is circulating at a depth of around 695 m (Table 5), considering an average geothermal gradient of 30°C per km. The chalcedony temperature and groundwater circulation depth were computed for all the wells during both sampling periods (Table 5).

In PRMS, 2019, for peri-urban shallow wells, the chalcedony temperature ranged between 8–32°C which indicates that the groundwater is circulating in a depth range of 280–1049 m, for urban shallow wells, it varied from 8–27°C, signifying a circulation depth range of 264–898 m and for deep wells, it varied between 34–44°C, revealing that the groundwater circulates within the depth range of 1129–1462 m.

In POMS, 2019, for peri-urban shallow wells, the chalcedony temperature ranged between 21–43°C which

**Table 5** Range of SiO<sub>2</sub>, Cl, TDS and chalcedony temperature

| PRMS, 2019                 |            |           |                         |                      |                          |
|----------------------------|------------|-----------|-------------------------|----------------------|--------------------------|
| Parameters                 | TDS (mg/l) | Cl (mg/l) | SiO <sub>2</sub> (mg/l) | Chalcedony Temp (°C) | Depth of circulation (m) |
| Peri-urban shallow samples | 440–704    | 14–80     | 30–50                   | 8–32                 | 280–1049                 |
| Urban shallow samples      | 432–1146   | 48–165    | 30–45                   | 8–27                 | 264–898                  |
| Urban deep samples         | 461–578    | 34–68     | 52–63                   | 34–44                | 1129–1462                |
| POMS, 2019                 |            |           |                         |                      |                          |
| Peri-urban shallow samples | 424–680    | 23–77     | 30–48                   | 21–43                | 695–1432                 |
| Urban shallow samples      | 603–1128   | 63–153    | 33–44                   | 26–39                | 855–1299                 |
| Urban deep samples         | 433–601    | 48–85     | 51–63                   | 46–57                | 1531–1895                |

indicates the depth range of 695–1432 m, for urban shallow wells, it varied from 26–39°C, signifying a depth range of 855–1299 m and for deep wells, it varied between 46–57°C, revealing a depth range of 1531–1895 m. Thus, it is quite evident from the data that the groundwater samples coming from deeper depth have higher content of silica, thereby, reflecting more rock-water interaction at relatively high temperature as compared to the one with lesser silica content.

Theoretically the approach of transforming silica concentration levels in groundwater to approximate depth to aquifers is robust for the following reasons:

- i. Temperature dependence of silica solubility in water has been extensively studied in labs and is very well understood.
- ii. Silica is available in abundance in rocks and over-burden material and is picked up by circulating groundwater due to water-rock interaction.
- iii. The intensity of water-rock interaction depends on water to rock ratio and temperature.
- iv. In a number of studies in geothermal and non-geothermal areas, a relationship has been found between the silica concentration levels and thermal anomalies.

However, it is noteworthy that the depth estimated using silica thermometry is just an estimate which needs to be taken in relative terms. Samples with higher concentration of dissolved silica definitely seem to have a deeper origin compared to the aquifer inferred to have lower silica levels. Observed large scale variations in silica concentration levels may be because of various reasons, such as changes in pH and other physico-chemical parameters in the aquifer; alkaline solutions will have higher solubility of silica; sub-surface precipitation of silica; mixing of other polymorphs of silica, such as, amorphous silica and Water to rock ratio and duration of water-rock interaction (Güleç 2005).

The  $SiO_2$  versus Cl and  $SiO_2$  versus TDS relationships were used for inferring the comparative influences of natural and anthropogenic factors in the process of solute acquisition. Chloride shows an inert nature in natural environment (Ellis 1970). Also, owing to its large ionic size, it usually do not involve in ion-exchange reactions in groundwater. The chloride concentration in groundwater is influenced by both rock-water interactions and anthropogenic factors, whereas groundwater acquires silica exclusively and unequivocally from water-rock interaction (Khan and Umar 2010). If water-rock interaction is solely responsible for contributing chloride, its concentration will not vary widely for a given silica concentration. Otherwise, the situation pinpoints towards anthropogenic influence (Khan et al. 2015b).

Considering this fact, chloride concentration was related with silica concentrations for all the groundwater samples

during both the seasons. Based on  $SiO_2$  vs. Cl plots for PRMS, 2019 (Fig. 12a) and POMS, 2019 (Fig. 12b), three major clusters i.e. I, II and III were identified. The samples falling in Cluster I show that for a narrow range of  $SiO_2$  values, Cl rises upto 165 mg/l in PRMS, 2019 and 153 mg/l in POMS, 2019. This reflects the anthropogenic influence on groundwater chemistry of these samples. The samples falling in Cluster II shows that with increasing values of  $SiO_2$ , Cl also increases revealing that both water-rock interaction and anthropogenic factors govern the groundwater chemical characteristics. The samples falling in Cluster III shows that for a narrow range of Cl,  $SiO_2$  rises upto 63 mg/l in PRMS, 2019 and 66 mg/l in POMS, 2019. This indicate that geogenic processes is regulating the groundwater chemistry of these samples.

The TDS and  $SiO_2$  relationship is very similar to that of  $SiO_2$  and Cl. A strong correlation indicates that interaction occurring between rock and water is the prime source of dissolved ions. On the contrary, a large variation in TDS for relatively narrow  $SiO_2$  range indicates their origin from different sources. Considering this fact, TDS concentration was correlated with silica concentrations for all the groundwater samples during both sampling periods. Based on  $SiO_2$  vs. TDS plots for PRMS and POMS, 2019 (Fig. 12c and d respectively)), three clusters i.e. Cluster I, II and III were identified. The samples falling in Cluster I show that for a narrow range of  $SiO_2$  values, TDS rises upto 1146 mg/l in PRMS, 2019 and 1128 mg/l in POMS, 2019. This indicates the role of anthropogenic factors on groundwater chemical characteristics. The samples falling in Cluster II depict a positive correlation between TDS and  $SiO_2$  in both the sampling periods i.e. with increasing values of  $SiO_2$ , TDS also increases, revealing that both geogenic and anthropogenic factors are regulating the groundwater chemistry. The samples falling in Cluster III shows that for a small range of TDS,  $SiO_2$  rises upto 63 mg/l in both sampling periods. The results reflect the role of geogenic processes in influencing the groundwater chemistry of these samples. Overall, based on  $SiO_2$  vs. TDS and  $SiO_2$  vs. Cl plots, it is inferred that the groundwater chemistry of samples falling in Cluster I is influenced by anthropogenic sources, Cluster II is influenced by both anthropogenic and geogenic factors and Cluster III is governed by geogenic factors mainly.

In the light of above results and discussion, a conceptual model of the major operative processes which are regulating the groundwater chemical characteristics in the area was prepared (Fig. 13). It was concluded that the resultant groundwater chemistry is the cumulative effect of varied geogenic processes viz. silicate weathering, ion exchange, groundwater-surface water interaction. Apart from geogenic processes, the groundwater chemistry has also been affected

**Fig. 12** (a-b) SiO<sub>2</sub> vs. Cl plots, (c-d) SiO<sub>2</sub> vs. TDS plots

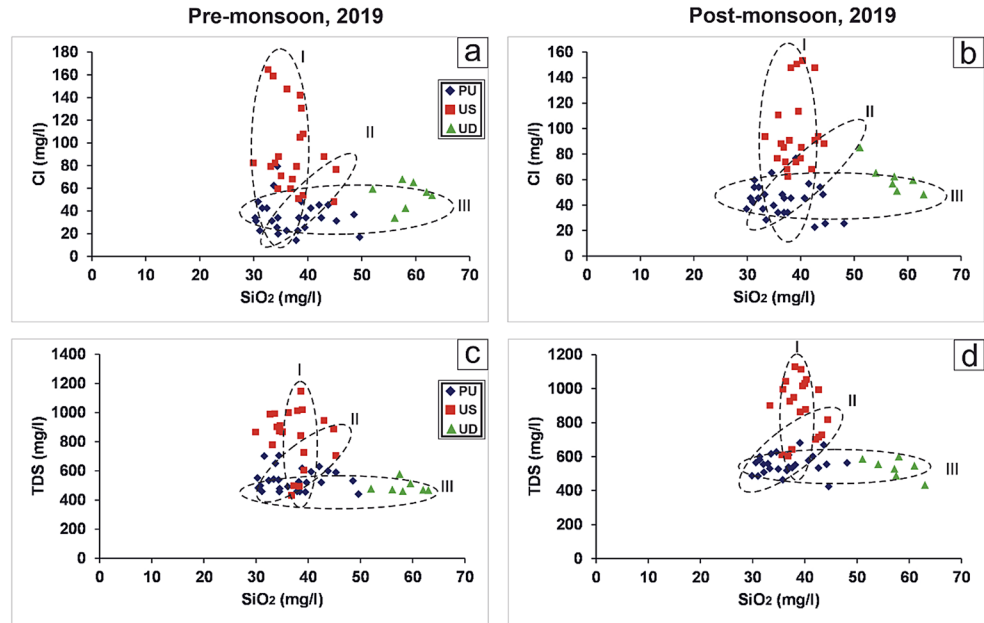
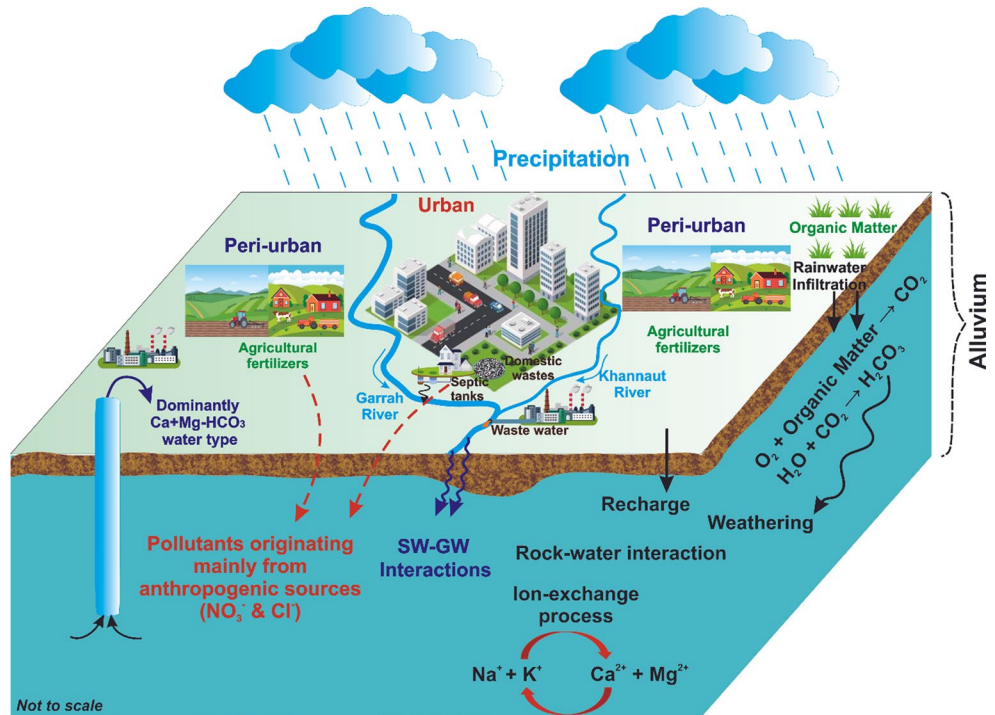


**Fig. 13** A conceptual model illustrating the dominant mechanisms governing the chemical attributes of groundwater in the investigated area



by anthropogenic sources like agricultural return flow, sewage disposal, septic tanks etc.

**Water quality assessment**

The presence of both natural and anthropogenic contaminants has created a rising concern on the availability of potable water with water quality emerging as one of the important facets of groundwater studies (Benaabidate et al. 2020). As the accessibility of potable water is crucial for

human existence, therefore, water quality assessment for its optimal utilization for drinking, irrigation and industrial use has been assessed.

The *groundwater drinking* appropriateness was examined by comparing the physico-chemical parameters with drinking water quality standards set by BIS (2012) and WHO (2017). Based on pH values, the groundwater was found to be of alkaline nature in both the sampling periods. As per hardness vs. TDS plots for PRMS, 2019 (Supplementary Fig. 3a) and POMS, 2019 (Supplementary Fig. 3b),

maximum number of samples lies in the category of fresh water and were hard in nature except for few urban shallow samples that lies just at the fresh-brackish interface and were very hard in nature. On an average, Na varied between 19 and 101 mg/l in PRMS, 2019 and 30 to 83 mg/l in POMS, 2019 for all type of groundwater samples. For  $\text{Na}^+$ , all samples remained within the threshold value of 200 mg/l established by WHO. The range of  $\text{Ca}^{2+}$  was between 19 and 101 mg/l in PRMS, 2019 and 30 to 83 mg/l in POMS, 2019. For  $\text{Ca}^{2+}$ , all type of samples adhered to the desirable limit (DL) which is 75 mg/l as outlined by BIS and WHO, except for 29% and 19% of urban shallow samples in PRMS, 2019 and POMS, 2019 respectively. High calcium content may result in abdominal ailments and may cause scaling and encrustation in water supply systems (Prasanth et al. 2012).  $\text{Mg}^{2+}$  varied between 8 and 66 mg/l in PRMS, 2019 and 9 to 58 mg/l in POMS, 2019 respectively. Regarding  $\text{Mg}^{2+}$ , majority of the peri-urban and urban deep samples adhered to the DL (30 mg/l) outlined by BIS and WHO whilst majority of urban shallow samples surpassed it in both sampling periods. At higher concentrations,  $\text{Mg}^{2+}$  may lead to laxative effects (WHO). The range of  $\text{HCO}_3^-$  is from 208 to 533 mg/l in PRMS, 2019 and 234 to 546 mg/l in POMS, 2019. A significant number of samples exceeded DL (200 mg/l) outlined by BIS for  $\text{HCO}_3^-$  in both the sampling periods. No known adverse health effect is associated with  $\text{HCO}_3^-$  (Shi et al. 2013). The range of  $\text{NO}_3^-$  is from not-detectable (nd) to 77 in PRMS, 2019 and nd to 100 mg/l in POMS, 2019. For  $\text{NO}_3^-$ , all the peri-urban shallow and urban deep samples adhered to the DL (45 mg/l) prescribed by BIS and WHO whilst majority of the urban shallow samples surpassed this limit in both the sampling periods. Consumption of high nitrate water may result in methemoglobinemia, goitre, gastric cancer, birth malformations etc. (Ward et al. 2018). The range of  $\text{F}^-$  is between nd to 0.88 mg/l in PRMS, 2019 while nd to 0.87 mg/l in POMS, 2019. All types of samples adhered to the DL (1 mg/l) outlined by BIS and WHO for  $\text{F}^-$ . Low fluoride concentration implies the occurrence of fluoride-bearing minerals in minimal amount in the study area. The values of  $\text{Cl}^-$  ranged between 14 and 164 mg/l in PRMS and 23 to 153 mg/l in POMS, 2019. For  $\text{Cl}^-$ , all types of samples adhered to the DL of 250 mg/l and 200 mg/l established by BIS and WHO respectively.  $\text{SO}_4^{2-}$  varied from 11 to 150 mg/l in PRMS, 2019 and 12 to 143 mg/l in POMS, 2019. All types

of samples adhered to the DL of 200 mg/l outlined by BIS and WHO for  $\text{SO}_4^{2-}$ . Further, it was observed that all the groundwater samples remained within the maximum permissible limit of BIS and WHO in both seasons. Overall, it was deciphered that majority of the groundwater samples were appropriate for drinking use, except for few shallow well samples of urban and peri-urban regions, in which  $\text{Ca}^+$ ,  $\text{Mg}^{2+}$ ,  $\text{HCO}_3^-$  and  $\text{NO}_3^-$  exceeds the DL.

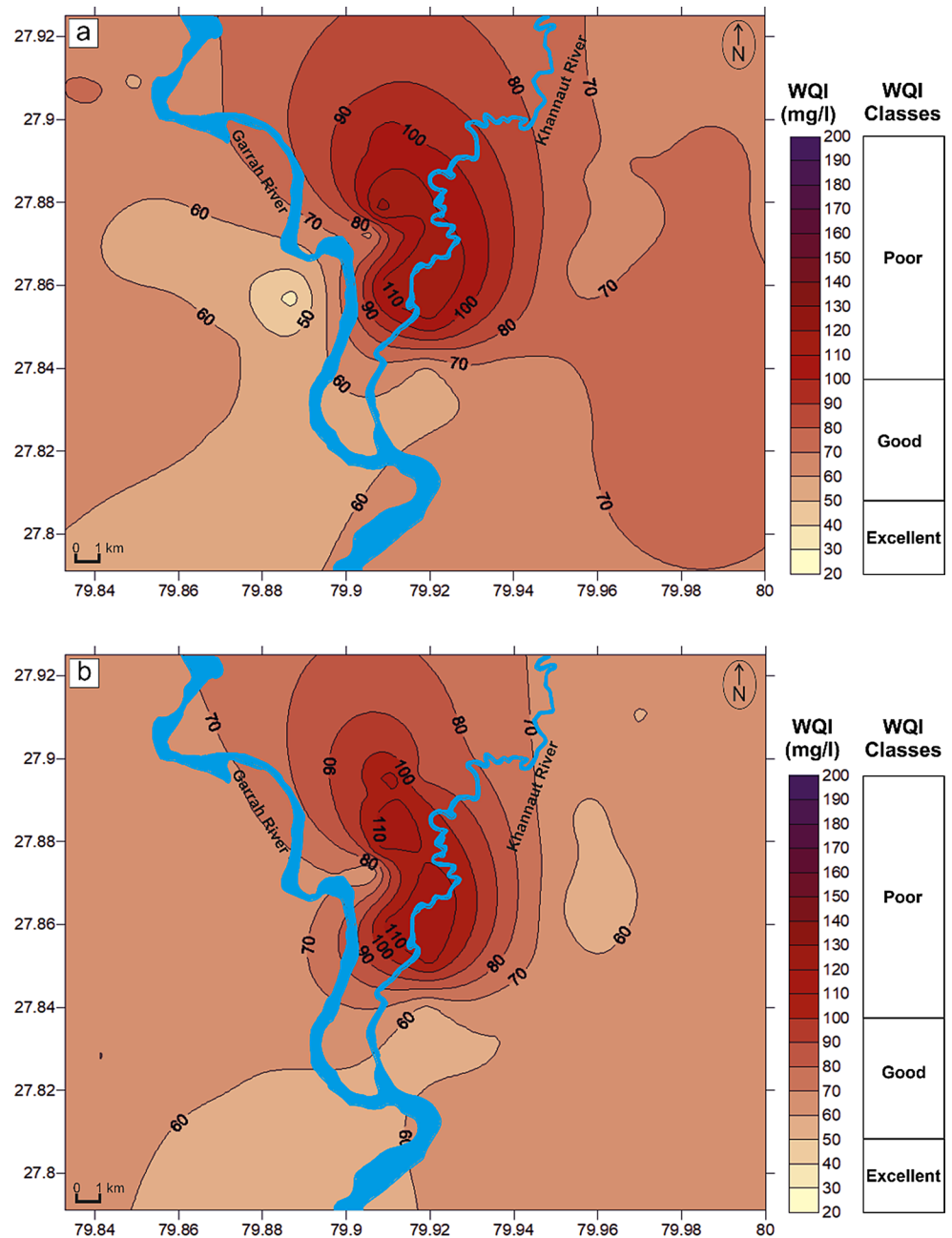
The groundwater drinking suitability also involved the utilization of *WQI*. Relative weight of chemical parameters in water quality index computation has been provided in Supplementary Table 4. Based on *WQI* values, all the peri-urban shallow samples were classified under good class, majority of the urban shallow samples fell under poor class and urban deep samples fell under excellent to good classes in both the sampling periods (Table 6), thereby, indicating that deeper depth groundwater samples were most suitable than the shallower ones. The shallow wells are relatively at higher risk of contamination than the deep wells as they usually tap the unconfined aquifer, where the water table tends to be shallow and thus more prone to contaminants. Various researchers have made similar observation in different parts of the Ganga basin (Ahmad et al. 2019; Rajmohan 2021). Further, the spatial distribution maps of *WQI* for PRMS, 2019 (Fig. 14a) and POMS, 2019 (Fig. 14b) depicts that groundwater samples collected from urban region possess higher *WQI* values as compared to the peri-urban regions. Groundwater in urban areas is particularly vulnerable to contamination due to the clustering of diverse pollution sources. These include septic tank leakages, domestic effluents from households and industries. Additionally, urban areas often have sewer systems that can leak or overflow during heavy rainfall, introducing sewage contaminants into the groundwater. Therefore, the concentration of pollution-generating activities in urban areas significantly heightens the likelihood of groundwater contamination.

The groundwater *irrigational suitability* was assessed by evaluating SAR, RSC and KR. The SAR values of samples in both sampling periods are given in Table 7. From SAR vs. EC plot of PRMS, 2019 (Fig. 15a) and POMS, 2019 (Fig. 15b), it was concluded that the groundwater and river water samples fell under two major classes i.e. C2S1 which represents medium salinity and low alkali water and C3S1 which represents high salinity and low alkali water in both the sampling periods. Groundwater and river water falling

**Table 6** Percentage of groundwater samples falling under different *WQI* classes

| <i>WQI</i> | Classes   | PRMS, 2019 |    |    | POMS, 2019 |    |    |
|------------|-----------|------------|----|----|------------|----|----|
|            |           | PU         | US | UD | PU         | US | UD |
| < 50       | Excellent | 0          | 10 | 57 | 0          | 0  | 14 |
| 50–100     | Good      | 100        | 19 | 43 | 100        | 38 | 86 |
| 100–200    | Poor      | 0          | 71 | 0  | 0          | 62 | 0  |

**Note:** PU denotes peri-urban shallow samples, US- urban shallow samples, UD- urban deep samples

**Fig. 14** WQI maps for (a) PRMS, 2019 and (b) POMS, 2019

under both the C2S1 and C3S1 categories is suitable for irrigation across most soil types, with minimal risk of reaching harmful levels of exchangeable sodium in the C3S1 category (Wilcox 1955). Overall, the water was found suitable for irrigational use.

The KR values of all types of groundwater samples and river water samples are summarised in Table 7. In PRMS, 2019, the variation in KR values is from 0.15 to 0.98 for peri-urban shallow, 0.36 to 0.98 for urban shallow, 0.50 to 0.98 for urban deep and 0.34 to 0.54 for river water samples. Similarly, in POMS 2019, the range extended from 0.19 to 0.96 for peri-urban shallow, 0.93 to 1.14 for urban shallow,

0.47 to 0.84 for urban deep and 0.43 to 0.81 for river water samples. It was observed that all peri-urban shallow, urban deep and river water samples across both sampling periods, as well as a significant proportion of urban shallow samples i.e. 100% in PRMS, 2019 and 95% in POMS 2019 had KR values below 1. This suggests that both surface and groundwater sources are suitable for irrigational use.

From the RSC values (Table 7), it was determined that a significant proportion of peri-urban shallow samples (88% in PRMS and 81% in POMS), urban shallow samples (90% in PRMS and 100% in POMS) and urban deep samples (86% each in PRMS and POMS) and all river samples

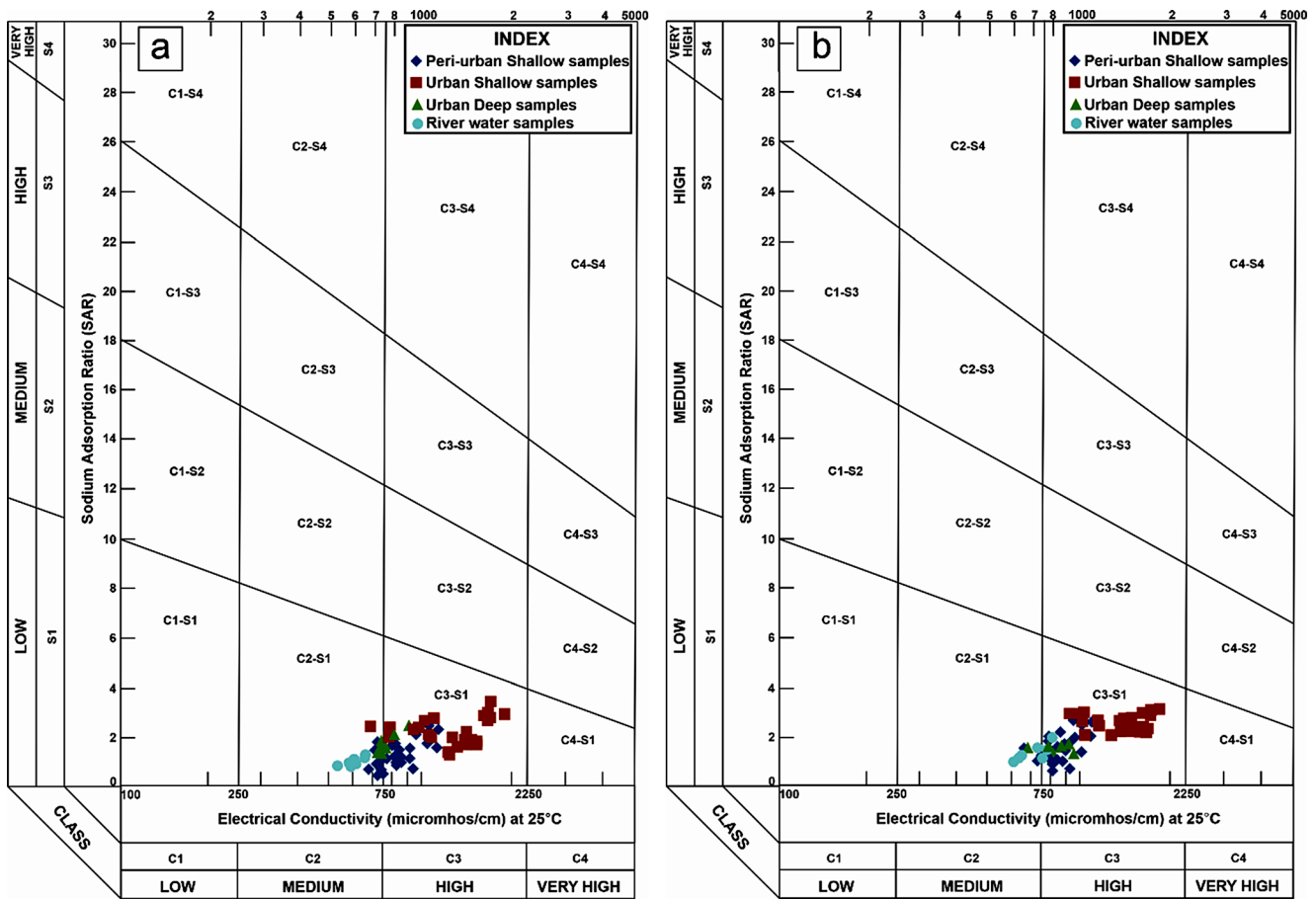


Fig. 15 USSSL diagrams for (a) PRMS, 2019 (b) POMS, 2019

consistently fell within the safe category ( $RSC < 1.25$ ) during both sampling periods and thus are suitable for irrigation use.

The *industrial suitability* of the groundwater was evaluated using L-SI in both the sampling periods (Table 7). During both sampling periods, it was noted that all peri-urban shallow, urban deep and river water samples, along with a considerable portion of urban shallow samples i.e. 62% in PRMS 2019 and 71% in POMS 2019), exhibited have  $L-SI < 0.8$ , thereby, indicating that they are non-corrosive in nature and thus are suitable for industrial uses.

### Conclusions

Hydrogeochemical investigations were carried out in peri-urban and urban regions of Shahjahanpur during PRMS and POMS, 2019 primarily to decipher the predominant geochemical processes that are affecting the groundwater system, to assess the seasonal variations in the physico-chemical parameters and to evaluate the water quality for different uses. Additionally, efforts were also undertaken to estimate the groundwater temperature and its corresponding

circulation depth while identifying the comparative contributions of geogenic processes and anthropogenic factors in regulating the groundwater chemistry through silica values. The major findings of the study are summarized below:

- Evaluation of the hydrogeochemical attributes revealed the cumulative effect of complex geogenic and anthropogenic influences on groundwater chemical characteristics. Statistical analysis through one-way ANOVA affirms that most of the hydrochemical parameters do not depict any substantial seasonal variations.
- Gibbs and other binary plots revealed that weathering of silicate is the key mechanism regulating the major ion chemistry. Additionally, the chloralkaline indices values revealed that ion exchange process is also regulating the chemical characteristics of groundwater to some extent. The comparable variations in most of the hydrogeochemical parameters between river and groundwater suggest that groundwater chemical characteristics is also getting affected by aquifer and river interaction. This can also be validated from the water table contour map which revealed the influent nature of the rivers.

**Table 7** Irrigational and industrial suitability indices of water samples in both sampling periods

|                                   | SN | PRMS, 2019               |       |      |                        | POMS, 2019               |       |      |                        |
|-----------------------------------|----|--------------------------|-------|------|------------------------|--------------------------|-------|------|------------------------|
|                                   |    | Irrigational suitability |       |      | Industrial suitability | Irrigational suitability |       |      | Industrial suitability |
|                                   |    | SAR                      | RSC   | KR   | L-SI                   | SAR                      | RSC   | KR   | L-SI                   |
| <b>Peri-urban shallow samples</b> | 1  | 1.12                     | 0.76  | 0.40 | 0.28                   | 1.45                     | 0.95  | 0.50 | 0.34                   |
|                                   | 2  | 1.44                     | 1.16  | 0.54 | 0.21                   | 1.67                     | 1.22  | 0.61 | 0.33                   |
|                                   | 3  | 1.21                     | 0.69  | 0.47 | 0.32                   | 1.46                     | 0.82  | 0.56 | 0.35                   |
|                                   | 4  | 1.47                     | 0.61  | 0.62 | 0.43                   | 1.72                     | 0.87  | 0.70 | 0.46                   |
|                                   | 5  | 2.48                     | 1.27  | 0.98 | 0.57                   | 2.52                     | 1.25  | 0.96 | 0.56                   |
|                                   | 6  | 1.79                     | 0.84  | 0.71 | 0.37                   | 2.01                     | 1.11  | 0.78 | 0.41                   |
|                                   | 7  | 1.13                     | 0.79  | 0.46 | 0.26                   | 1.53                     | 1.14  | 0.61 | 0.3                    |
|                                   | 8  | 1.72                     | 0.60  | 0.66 | 0.47                   | 1.84                     | 1.16  | 0.69 | 0.43                   |
|                                   | 9  | 2.14                     | 1.51  | 0.88 | 0.39                   | 2.17                     | 1.41  | 0.85 | 0.4                    |
|                                   | 10 | 0.67                     | 0.47  | 0.26 | 0.19                   | 1.49                     | 1.19  | 0.58 | 0.23                   |
|                                   | 11 | 2.31                     | 0.39  | 0.81 | 0.73                   | 2.6                      | 0.79  | 0.89 | 0.66                   |
|                                   | 12 | 1.05                     | 0.52  | 0.32 | 0.22                   | 1.17                     | 0.39  | 0.36 | 0.29                   |
|                                   | 13 | 0.46                     | 0.47  | 0.15 | 0.13                   | 0.57                     | 0.04  | 0.19 | 0.22                   |
|                                   | 14 | 1.12                     | 0.10  | 0.36 | 0.34                   | 1.21                     | 0.36  | 0.39 | 0.33                   |
|                                   | 15 | 0.57                     | 0.39  | 0.18 | 0.2                    | 0.66                     | -0.06 | 0.21 | 0.32                   |
|                                   | 16 | 1.77                     | 1.62  | 0.69 | 0.25                   | 1.99                     | 1.67  | 0.76 | 0.33                   |
|                                   | 17 | 0.9                      | 0.79  | 0.33 | 0.23                   | 1.02                     | 0.50  | 0.37 | 0.3                    |
|                                   | 18 | 0.93                     | -0.43 | 0.31 | 0.57                   | 1.41                     | 0.28  | 0.47 | 0.54                   |
|                                   | 19 | 0.96                     | 0.60  | 0.29 | 0.26                   | 1.36                     | 0.65  | 0.41 | 0.31                   |
|                                   | 20 | 0.92                     | 0.34  | 0.30 | 0.26                   | 1.37                     | 0.47  | 0.45 | 0.35                   |
|                                   | 21 | 1.54                     | 1.01  | 0.57 | 0.32                   | 1.82                     | 1.30  | 0.68 | 0.41                   |
|                                   | 22 | 0.53                     | 0.31  | 0.16 | 0.2                    | 0.84                     | 0.44  | 0.25 | 0.28                   |
|                                   | 23 | 1.54                     | -0.23 | 0.45 | 0.51                   | 1.91                     | -0.04 | 0.55 | 0.49                   |
|                                   | 24 | 1.11                     | 1.08  | 0.36 | 0.24                   | 0.97                     | 0.55  | 0.30 | 0.22                   |
|                                   | 25 | 0.71                     | -0.23 | 0.18 | 0.28                   | 1.1                      | 0.30  | 0.31 | 0.35                   |
|                                   | 26 | 1.76                     | 1.06  | 0.63 | 0.42                   | 2.71                     | 2.60  | 0.96 | 0.32                   |
| <b>Urban shallow samples</b>      | 27 | 1.86                     | -1.00 | 0.52 | 0.83                   | 2.29                     | -0.47 | 0.63 | 0.8                    |
|                                   | 28 | 2.05                     | 0.06  | 0.55 | 0.49                   | 2.03                     | 0.33  | 0.54 | 0.46                   |
|                                   | 29 | 1.72                     | -1.32 | 0.47 | 0.87                   | 2.7                      | 0.06  | 0.72 | 0.71                   |
|                                   | 30 | 1.32                     | -0.84 | 0.36 | 0.52                   | 2.04                     | -0.23 | 0.54 | 0.61                   |
|                                   | 31 | 1.68                     | 0.06  | 0.45 | 0.42                   | 2.19                     | 1.02  | 0.60 | 0.43                   |
|                                   | 32 | 2.81                     | 0.73  | 0.73 | 0.61                   | 2.2                      | 0.46  | 0.53 | 0.51                   |
|                                   | 33 | 2.92                     | -1.32 | 0.76 | 1.13                   | 2.89                     | -1.64 | 0.77 | 1.3                    |
|                                   | 34 | 3.41                     | -0.73 | 0.90 | 1.22                   | 3.09                     | -1.58 | 0.86 | 1.46                   |
|                                   | 35 | 2.74                     | 0.97  | 0.69 | 0.47                   | 2.46                     | 0.67  | 0.62 | 0.48                   |
|                                   | 36 | 2.42                     | 0.90  | 0.93 | 0.63                   | 2.89                     | 0.95  | 1.00 | 0.74                   |
|                                   | 37 | 2.04                     | 0.12  | 0.79 | 0.86                   | 2.95                     | 0.68  | 1.14 | 0.85                   |
|                                   | 38 | 2.14                     | -0.23 | 0.60 | 0.56                   | 2.68                     | 0.86  | 0.76 | 0.57                   |
|                                   | 39 | 1.79                     | -1.19 | 0.51 | 0.87                   | 2.15                     | -0.36 | 0.60 | 0.75                   |
|                                   | 40 | 1.75                     | -0.31 | 0.46 | 0.47                   | 2.24                     | 1.05  | 0.62 | 0.45                   |
|                                   | 41 | 2.77                     | 1.61  | 0.73 | 0.43                   | 2.33                     | 0.22  | 0.56 | 0.52                   |
|                                   | 42 | 2.7                      | -1.00 | 0.72 | 1.03                   | 2.93                     | -1.45 | 0.77 | 1.19                   |
|                                   | 43 | 2.93                     | -1.88 | 0.77 | 1.4                    | 3.03                     | -1.64 | 0.85 | 1.48                   |
|                                   | 44 | 2.59                     | 1.32  | 0.72 | 0.51                   | 2.6                      | 0.78  | 0.67 | 0.47                   |
|                                   | 45 | 2.34                     | 1.11  | 0.83 | 0.57                   | 2.75                     | 1.08  | 0.94 | 0.64                   |
|                                   | 46 | 2.31                     | 0.15  | 0.85 | 0.79                   | 2.66                     | 0.50  | 0.97 | 0.76                   |
|                                   | 47 | 1.97                     | 0.15  | 0.59 | 0.57                   | 2.61                     | 0.81  | 0.75 | 0.57                   |

Table 7 (continued)

|                           | SN | PRMS, 2019               |      |      |                        | POMS, 2019               |      |      |                        |
|---------------------------|----|--------------------------|------|------|------------------------|--------------------------|------|------|------------------------|
|                           |    | Irrigational suitability |      |      | Industrial suitability | Irrigational suitability |      |      | Industrial suitability |
|                           |    | SAR                      | RSC  | KR   | L-SI                   | SAR                      | RSC  | KR   | L-SI                   |
| <b>Urban deep samples</b> | 48 | 2.47                     | 1.48 | 0.98 | 0.49                   | 2.23                     | 1.59 | 0.84 | 0.44                   |
|                           | 49 | 1.77                     | 0.98 | 0.69 | 0.46                   | 1.99                     | 1.24 | 0.76 | 0.44                   |
|                           | 50 | 1.48                     | 0.69 | 0.57 | 0.47                   | 1.72                     | 0.82 | 0.66 | 0.52                   |
|                           | 51 | 1.38                     | 0.63 | 0.50 | 0.45                   | 1.67                     | 0.23 | 0.57 | 0.66                   |
|                           | 52 | 1.69                     | 0.74 | 0.58 | 0.5                    | 2.15                     | 1.08 | 0.74 | 0.55                   |
|                           | 53 | 1.63                     | 0.63 | 0.59 | 0.52                   | 1.41                     | 0.92 | 0.47 | 0.36                   |
| <b>River samples</b>      | 54 | 2.12                     | 0.79 | 0.86 | 0.68                   | 1.99                     | 0.76 | 0.71 | 0.56                   |
|                           | 55 | 1.00                     | 0.45 | 0.41 | 0.29                   | 1.91                     | 0.82 | 0.81 | 0.50                   |
|                           | 56 | 0.85                     | 0.58 | 0.34 | 0.27                   | 1.39                     | 0.71 | 0.56 | 0.42                   |
|                           | 57 | 1.23                     | 0.00 | 0.54 | 0.52                   | 1.18                     | 0.39 | 0.50 | 0.45                   |
|                           | 58 | 0.99                     | 0.15 | 0.40 | 0.35                   | 1.49                     | 0.55 | 0.58 | 0.48                   |
|                           | 59 | 0.95                     | 0.37 | 0.43 | 0.39                   | 1.14                     | 0.23 | 0.47 | 0.49                   |
|                           | 60 | 1.04                     | 0.26 | 0.45 | 0.27                   | 0.95                     | 0.15 | 0.43 | 0.44                   |
|                           | 61 | 0.85                     | 0.15 | 0.34 | 0.28                   | 1.08                     | 0.42 | 0.48 | 0.44                   |

- The results obtained from silica geothermometry implies that groundwater coming from deeper depths have higher silica content, indicating greater extent of water-rock interaction at relatively higher temperatures. Relationships of SiO<sub>2</sub> vs. TDS and SiO<sub>2</sub> vs. Cl confirms the impact of both geogenic and anthropogenic influences in governing the groundwater chemical characteristics.
- The groundwater suitability assessment revealed that maximum samples were appropriate for drinking use except for few, in which Ca, Mg, HCO<sub>3</sub> and NO<sub>3</sub> exceeds the desirable limits. WQI values revealed comparatively poor groundwater quality in urban region which might be attributed to the leakages from domestic effluents, sewers, septic tank, etc. Based on the results of irrigational and industrial water quality indices, most of the samples were found appropriate for these uses.

Despite employing diverse methodologies and making diligent efforts to enhance the comprehensiveness of this work, it cannot be deemed entirely sufficient in all respects. It still offers avenues for researchers on aspects like isotopic studies which will be helpful in obtaining a more thorough understanding of water quality problems, origin of the circulating waters, inter-relations between surface waters and groundwaters etc. Overall, it is expected that the insights derived from this study will be helpful in understanding the hydrogeochemical conditions of Shahjahanpur. This knowledge will be valuable for researchers, policy-makers, and stakeholders in devising precise strategies to conserve and improve the quality of groundwater resources.

**Supplementary Information** The online version contains supplementary material available at <https://doi.org/10.1007/s40899-024-01090-7>.

**Acknowledgements** The authors gratefully acknowledge the editors and reviewers for their valuable suggestions and comments which have improved this manuscript substantially. The first author would also like to acknowledge the financial assistance received in the form of a Non-NET fellowship from the University Grant Commission (UGC), New Delhi. The authors are also thankful to the Chairperson, Department of Geology, Aligarh Muslim University (A.M.U.), Aligarh, for providing basic laboratory facilities in the Geochemical lab.

**Author contributions** All authors Rashid Umar and Ilma Arshad contributed to the study conception and design. Material preparation, data collection and analysis were performed by Ilma Arshad. The first draft of the manuscript was written by Ilma Arshad. All authors read and approved the final manuscript.

**Funding** The first author had received funding in the form of University Grant Commission (UGC) Non-NET fellowship.

**Data availability** All data generated or analyzed during this study are included in the manuscript.

## Declarations

**Conflict of interest** The authors have no conflict of interest to declare that are relevant to the content of this article.

## References

- Ahmad S, Umar R, Arshad I (2019) Groundwater quality appraisal and its hydrogeochemical characterization-Mathura City, Western Uttar Pradesh. *J Geol Soc India* 94(6):611–623. <https://doi.org/10.1007/s12594-019-1368-5>
- Amiri V, Bhattacharya P, Nakhaei M (2021) The hydrogeochemical evaluation of groundwater resources and their suitability for agricultural and industrial uses in an arid area of Iran. *Groundw Sustain Dev* 12:100527. <https://doi.org/10.1016/j.gsd.2020.100527>
- Annapoorna H, Janardhana MR (2015) Assessment of groundwater quality for drinking purpose in rural areas surrounding a defunct copper mine. *Aquat Procedia* 4:685–692



- APHA (1992) Standard methods for the examination of Water and Wastewater, 16th edition, American Public Health Association, Washington, D.C
- Arshad I, Umar R (2020) Status of urban hydrogeology research with emphasis on India Hydrogeol. J 28(2):477–490
- Arshad I, Umar R (2023) Status of heavy metals and metalloid concentrations in water resources and associated health risks in parts of Indo-Gangetic plain, India Groundw. Sustain Dev 23:101047
- Arumugam M, Karthikeyan S, Thangaraj K, Kulandaisamy P, Sundaram B, Ramasamy K, Vellaikannu A, Velmayil P (2021) Hydrogeochemical analysis for groundwater suitability appraisal in sivagangai, an economically backward District of Tamil Nadu. J Geol Soc India 97:789–798. <https://doi.org/10.1007/s12594-021-1761-8>
- Bai X, Tian X, Li J, Wang X, Li Y, Zhou Y (2022) Assessment of the hydrochemical characteristics and formation mechanisms of Groundwater in a typical alluvial-Proluvial Plain in China: an Example from Western. Yongqing Cty Water 14(15):2395
- Benaabidate L, Zian A, Sadki O (2020) Hydrochemical characteristics and quality assessment of water from different sources in Northern Morocco. In: Mukherjee (eds.) Global Groundwater: Source, Scarcity, Sustainability, Security, Solutions. Elsevier, ISBN: 978-0-12-818172-0, pp. 261–274
- BIS (2012) Specification for drinking water, IS: 10500:91. Bureau of Indian Standards, New Delhi, India
- CGWB (2013) District Ground Water Brochure of Shahjahanpur District, UP. Central Ground Water Board, p 25
- CGWB (2021) Aquifer Mapping and Management of Ground Water resources Shahjahanpur District, Uttar Pradesh. Central Ground Water Board Department of Water Resources, River Development and Ganga Rejuvenation, Ministry of Jal Shakti Government of India. Northern Region, Lucknow, p 174
- Ellis AJ (1970) Quantitative interpretation of chemical characteristics of hydrothermal systems. Geothermics 2:516–527
- Fisher SR, Mullican WF (1997) Hydrogeochemical evolution of sodium sulphate and sodium-chloride groundwater beneath the northern Chihuahua desert, Trans-Pecos, Texas, U.S.A. Hydrogeol J 5:4–16. <https://doi.org/10.1007/s100400050102>
- Fournier RO, Potter IIRW (1982) A revised and expanded silica geothermometer. Bull Geotherm Resour Counc 11:3–12
- Ganiyu SA, Adefarati IK, Akinyemi AA (2023) Assessment of quality status of raw and treated water from Erelu waterworks using data of routine monitoring parameters (2018–2020). Sustain Water Resour Manag 9:173. <https://doi.org/10.1007/s40899-023-00951-x>
- Gibbs RJ (1970) Mechanisms controlling world water chemistry. Sci J 170:795–840
- Giordano M (2009) Global groundwater? Issues and solutions. Annu Rev Environ Resour 34:153–178
- Güleç N (2005) Applications of Geothermometry, Geothermal Geochemistry and some New Geothermal approaches. Dokuz Eylül University, GeothermalEnergy Research and Application Center (GERAC)
- Hem JD (1985) Study and interpretations of chemical characteristics of natural water. USGS Water Supply Paper No 2254:263
- Hounslow AW (1995) Water Quality Data Analysis and Interpretation. CRC, Florida
- Howard KWF, Gelo KK (2002) Intensive groundwater use in urban areas: the case of megacities. In Intensive use of groundwater: challenges and opportunities. pp. 484
- Karant K (1987) Groundwater assessment: Development and Management. Tata McGraw-Hill, New Delhi. ISBN-13: 978-0-07-451712-3
- Khan MMA, Umar R (2010) Significance of silica analysis in groundwater in parts of Central Ganga Plain, Uttar Pradesh, India. Curr Sci 98(9):1237–1240
- Khan S, Khan S, Khan MN, Khan AA (2015a) Pre and post monsoon variation in Physico-chemical characteristics in groundwater quality of Shahjahanpur the town of martyrs, India: a case study. Int Res J Environ Sci 4(10):107–114
- Khan A, Umar R, Khan HH (2015b) Significance of silica in identifying the processes affecting groundwater chemistry in parts of Kali watershed, Central Ganga Plain, India. Appl Water Sci 5:65–72. <https://doi.org/10.1007/s13201-014-0164-z>
- Khan MYA, Khan B, Chakrapani GJ (2016) Assessment of spatial variations in water quality of Garra River at Shahjahanpur, Ganga Basin, India. Arab J Geosci 9:516. <https://doi.org/10.1007/s12517-016-2551-2>
- Khokhar LAK, Khuhawar MY, Khuhawar TMJ, Lanjwani MF, Arain GM, Khokhar FM, Khaskheli MI (2023) Spatial variability and hydrochemical quality of groundwater of Hyderabad Rural, Sindh, Pakistan. Sustainable Water Resour Manage 9(5):164. <https://doi.org/10.1007/s40899-023-00944-w>
- Lapworth D, Boving T, Brauns B, Dottridge J, Hynds P, Kebede S, Kreamer D, Misstear B, Mukherjee A, Re V, Sorensen J (2023) Groundwater quality: global challenges, emerging threats and novel approaches. Hydrogeol J 31(1):15–18. <https://doi.org/10.1007/s10040-022-02542-0>
- Li X, Wu H, Qian H, Gao Y (2018) Groundwater Chemistry regulated by hydrochemical processes and geological structures: a Case Study in Tongchuan. China Water 10(3):338. <https://doi.org/10.3390/w10030338>
- Li P, He X, Guo W (2019) Spatial groundwater quality and potential health risks due to nitrate ingestion through drinking water: a case study in Yan'an City on the Loess Plateau of northwest China. Hum Ecol Risk Assess 25(1–2):11–31. <https://doi.org/10.1080/10807039.2018.1553612>
- Madhav S, Ahmad A, Kumar A, Kushawaha J, Singh P, Mishra PK (2018) Geochemical assessment of groundwater quality for its suitability for drinking and irrigation purpose in rural areas of Sant Ravidas Nagar (Bhadohi), Uttar Pradesh Geol. ecol Landsc 2(2):127–136
- Marchand D, Rayan MC, Bethune DN, Chu A (2002) Groundwater-Surface Water Interaction and Nitrate Origin in Municipal Water Supply Aquifers, Sanjose, Costa Rica
- Marghade D, Malpe DB, Zade AB (2011) Geochemical characterization of groundwater from North-eastern part of Nagpur urban, Central India. Environ Earth Sci 62(7):1419–1430. <https://doi.org/10.1007/s12665-010-0627-y>
- Mays LW (2013) Groundwater resources sustainability: past, present, and future. Water Resour Manag 27:4409–4424. <https://doi.org/10.1007/s11269-013-0436-7>
- Misstear BDR, Ruz Vargas C, Lapworth D, Ouedraogo I, Podgorski J (2022) A global perspective on assessing groundwater quality. Hydrogeol J. <https://doi.org/10.1007/s10040-022-02461-0>
- Mukherjee A (2018) Groundwater of South Asia. Springer Singapore ISBN:978-981-10-3888-4. pp. 799
- Mukherjee A, Scanlon BR, Aureli A, Langan S, Guo H, McKenzie AA (2021) Global groundwater: source, scarcity, sustainability, security, and solutions. In Mukherjee (eds.): Global groundwater: source, scarcity, sustainability, security, and solutions. ISBN: 978-0-12-818172-0. pp. 639
- NITI Ayog (2018) Composite Water Management Index- A tool for water management. National Institution for Transforming India (NITI) Ayog, Government of India pp.177
- Nzama SM, Kanyerere TOB, Mapoma HWT (2021) Using groundwater quality index and concentration duration curves for classification and protection of groundwater resources: relevance of groundwater quality of reserve determination, South Africa. Sustain Water Resour Manag 7(31):1–11. <https://doi.org/10.1007/s40899-021-00503-1>

- Okiongbo KS, Akpofure E (2014) Identification of hydrogeochemical processes in groundwater using major ion chemistry: a case study of Yenagoa and environs, southern Nigeria Glob. J Geol Sci 12:39–52
- Parween S, Siddique NA, Diganta MTM, Olbert AI, Uddin MG (2022) Assessment of urban river water quality using modified NSF water quality index model at Siliguri city, West Bengal, India Environ. Sustain Indic 16:100202
- Pazand K, Khosravi D, Ghaderi MR, Rezvanzadeh MR (2018) Identification of the hydrogeochemical processes and assessment of groundwater in a semi-arid region using major ion chemistry: a case study of Ardestan basin in Central Iran. Groundw Sustain Dev 6:245–254. <https://doi.org/10.1016/j.gsd.2018.01.008>
- Prasanth SV, Magesh NS, Jitheshlal KV, Chandrasekar N, Gangadhar KJAWS (2012) Evaluation of groundwater quality and its suitability for drinking and agricultural use in the coastal stretch of Alappuzha District, Kerala, India. Appl Water Sci 2(3):165–175. <https://doi.org/10.1007/s13201-012-0042-5>
- Rajmohan N (2021) Application of water quality index and chemometric methods on contamination assessment in the shallow aquifer, Ganges River basin, India. Environ Sci Pollut Res 28(18):23243–23257. <https://doi.org/10.1007/s11356-020-12270-1>
- Rajmohan N, Amarasinghe U (2016) Groundwater quality issues and management in Ramganga Sub-basin. Environ Earth Sci 75(12):1–14
- Rajmohan N, Elango L (2004) Identification and evolution of hydrogeochemical processes in an area of the Palar and Cheyyar River Basin, Southern India. Environ Geol 46:47–61. <https://doi.org/10.1007/s00254-004-1012-5>
- Raju NJ, Shukla UK, Ram P (2011) Hydrogeochemistry for the assessment of groundwater quality in Varanasi: a fast-urbanizing center in Uttar Pradesh, India Environ. Monit Assess 173(1–4):279–300
- Richards LA (1954) Diagnosis and improvement of saline and Alkali soils. US Department of Agriculture, Washington DC, p 160
- Rouxel M, Molénat J, Ruiz L, Legout C, Fauchoux M, Gascuel-Oudou C (2011) Seasonal and spatial variation in groundwater quality along the hillslope of an agricultural research catchment (Western France). Hydrol Process 25(6):831–841
- Saba N (2016) Segregation of various types of contamination in urban groundwater of Moradabad city and suggestion for its suitable remediation. Aligarh Muslim University
- Saba N, Umar R (2016) Hydrogeochemical assessment of Moradabad city, an important industrial town of Uttar Pradesh, India. Sustain Water Resour Manag 2:217–236. <https://doi.org/10.1007/s40899-016-0053-8>
- Sajib AM, Diganta MT, Rahman A, Dabrowski T, Olbert AI, Uddin MG (2023) Developing a novel tool for assessing the groundwater incorporating water quality index and machine learning approach Groundw. Sustain Dev 23:101049
- Schoeller H (1967) Geochemistry of groundwater. An international guide for research and practice. UNESCO. pp.1–18
- Shaibur MR, Ahmmed I, Sarwar S, Karim R, Hossain MM, Islam MS, Shah MS, Khan AS, Akhtar F, Uddin MG, Rahman MM (2023) Groundwater quality of some parts of coastal bhola district, Bangladesh: exceptional evidence Urban Sci. 7(3): 71
- Shi J, Ma R, Liu J, Zhang Y (2013) Suitability assessment of deep groundwater for drinking, irrigation and industrial purposes in Jiaozuo City, Henan Province, North China. Chin Sci Bull 58(25):3098–3110. <https://doi.org/10.1007/s11434-013-5952-6>
- Singh A, Raju A, Chandniha SK, Singh L, Tyagi I, Karri RR, Kumar A (2023) Hydrogeochemical characterization of groundwater and their associated potential health risks. Environ Sci Pollut Res Int 30(6):14993–15008. <https://doi.org/10.1007/s11356-022-23222-2>
- Sinha H, Rai SC, Kumar S (2023) Post-monsoon groundwater hydrogeochemical characterization and quality assessment using geospatial and multivariate analysis in Chhotanagpur Plateau, India. Environ Dev Sustain. <https://doi.org/10.1007/s10668-023-03459-8>
- Swanberg CA, Morgan P (1978) The linear relation between temperatures based on the silica content of groundwater and regional heat flow: a new heat flow map of the United. State Pure Appl Geophys 117(1–12):227–241
- Todd DK, Mays LW (2005) Groundwater Hydrology. 3rd ed. John Wiley and Sons, United States of America. ISBN: 978-81-265-3003-8
- Uddin MG, Nash S, Olbert AI (2021) A review of water quality index models and their use for assessing surface water quality. Ecol Indic 122:107218
- Uddin MG, Nash S, Rahman A, Olbert AI (2022) A comprehensive method for improvement of water quality index (WQI) models for coastal water quality assessment. Water Res 219:118532
- Uddin MG, Diganta MT, Sajib AM, Rahman A, Nash S, Dabrowski T, Ahmadian R, Hartnett M, Olbert AI (2023a) Assessing the impact of COVID-19 lockdown on surface water quality in Ireland using advanced Irish Water Quality Index (IEWQI) Model Environ. Pollut 336:122456
- Uddin MG, Nash S, Rahman A, Olbert AI (2023b) A sophisticated model for rating water quality Sci. Total Environ 868:161614
- Uddin MG, Jackson A, Nash S, Rahman A, Olbert AI (2023c) Comparison between the WFD approaches and newly developed water quality model for monitoring transitional and coastal water quality in Northern Ireland. Sci Total Environ 901:165960
- Vasconcelos HC, Fernandez-Perez BM, Gonzalez S, Souto RM, Santana JJ (2015) Characterization of the corrosive action of mineral waters from thermal sources: a case study at Azores Archipelago. Portugal Water 7(7):3515–3530. <https://doi.org/10.3390/w7073515>
- Wali SU, Umar KJ, Abubakar SD, Ifabiyi IP, Dankani IM, Shera IM, Yauri SG (2019) Hydrochemical characterization of shallow and deep groundwater in Basement Complex areas of southern Kebbi State, Sokoto Basin, Nigeria. Appl Water Sci 9:169. <https://doi.org/10.1007/s13201-019-1042-5>
- Ward MH, Jones RR, Brender JD, De Kok TM, Weyer PJ, Nolan BT, Villanueva CM, Van Breda SG (2018) Drinking water nitrate and human health: an updated review. Int. J. Environ. Health Res 15(7), pp.1557. <https://doi.org/10.3390/ijerph15071557>
- WHO (2017) Guidelines for drinking-water quality 4th ed. Incorporating the first addendum. World Health Organization Geneva, Switzerland. ISBN: 978-92-4-154995-0
- Wilcox LV (1955) Classification and use of irrigation waters. US Department of Agriculture., Washington DC., p 19. Circular 969
- Yang Q, Li Z, Ma H, Wang L, Martin JD (2016) Identification of the hydrogeochemical processes and assessment of groundwater quality using classic integrated geochemical methods in the Southeastern part of Ordos basin, China. Environ Pollut 218:879–888. <https://doi.org/10.1016/j.envpol.2016.08.017>
- Zhang X, Miao J, Hu BX, Liu H, Zhang H, Ma Z (2017) Hydrogeochemical characterization and groundwater quality assessment in intruded coastal brine aquifers Laizhou Bay, China. Environ Sci Pollut Res 24:21073–21090. <https://doi.org/10.1007/s11356-017-9641-x>

**Publisher's Note** Springer Nature remains neutral with regard to jurisdictional claims in published maps and institutional affiliations.

Springer Nature or its licensor (e.g. a society or other partner) holds exclusive rights to this article under a publishing agreement with the author(s) or other rightsholder(s); author self-archiving of the accepted manuscript version of this article is solely governed by the terms of such publishing agreement and applicable law.